Applications of Satellite Remote Sensing of Nighttime Light Observations: Advances, Challenges, and Perspectives

Min Zhao [1,2,3,4], **Yuyu Zhou** [1,*], **Xuecao Li** [1], **Wenting Cao** [1], **Chunyang He** [5], **Bailang Yu** [6], **Xi Li** [7], **Christopher D. Elvidge** [8], **Weiming Cheng** [3] **and Chenghu Zhou** [3,4]

1   Department of Geological and Atmospheric Sciences, Iowa State University, Ames, IA 50011, USA
2   School of Geographic and Oceanographic Sciences, Nanjing University, Nanjing 210023, China
3   State Key Laboratory of Resources and Environmental Information Systems,
    Institute of Geographic Sciences and Natural Resources Research, Chinese Academy of Sciences,
    Beijing 100101, China
4   Collaborative Innovation Center of South China Sea Studies, Nanjing 210023, China
5   Center for Human-Environment System Sustainability, State Key Laboratory of Earth Surface Processes and
    Resource Ecology, Faculty of Geographical Science, Beijing Normal University, Beijing 100875, China
6   Key Laboratory of Geographic Information Science (Ministry of Education), East China Normal University,
    Shanghai 200241, China
7   State Key Laboratory of Information Engineering in Surveying, Mapping and Remote Sensing,
    Wuhan University, Wuhan 430079, China
8   Earth Observation Group, Payne Institute, Colorado School of Mines, 1500 Illinois St., Golden,
    CO 80401, USA
*   Correspondence: yuyuzhou@iastate.edu; Tel.: +1-515-294-2842

Abstract: Nighttime light observations from remote sensing provide us with a timely and spatially explicit measure of human activities, and therefore enable a host of applications such as tracking urbanization and socioeconomic dynamics, evaluating armed conflicts and disasters, investigating fisheries, assessing greenhouse gas emissions and energy use, and analyzing light pollution and health effects. The new and improved sensors, algorithms, and products for nighttime lights, in association with other Earth observations and ancillary data (e.g., geo-located big data), together offer great potential for a deep understanding of human activities and related environmental consequences in a changing world. This paper reviews the advances of nighttime light sensors and products and examines the contributions of nighttime light remote sensing to perceiving the changing world from two aspects (i.e., human activities and environmental changes). Based on the historical review of the advances in nighttime light remote sensing, we summarize the challenges in current nighttime light remote sensing research and propose four strategic directions, including: Improving nighttime light data; developing a long time series of consistent nighttime light data; integrating nighttime light observations with other data and knowledge; and promoting multidisciplinary and interdisciplinary analyses of nighttime light observations.

Keywords: nighttime light; advances; challenges; strategic directions; review

1. Introduction

Accelerated human modifications of the landscape and human-driven climate changes are profoundly affecting the processes on the Earth surface, locally and globally, and creating a variety of challenges for scientists and policy makers to understand and address the global change and

consequences [1,2]. At the same time, new geographical concepts, datasets, tools, and techniques are emerging to advance our understanding of topics such as urbanization, environmental change, sustainability, and global change. The footprint of human beings is undoubtedly a salient indicator of the human impacts on both the environment and ecosystems [3]. Imageries of the Earth's surface observed from space show great potentials in monitoring, analyzing, evaluating, and predicting the unprecedented changes that occur on the Earth's surface, making it possible for us to quantify and track the dynamics of human activity and its environmental impacts [4]. Satellite remote sensing will continue to play an important role for a comprehensive understanding of changes faced by the Earth and human in the 21st century.

As one of the hallmarks of human footprints on the Earth's surface [5], the nocturnal lighting measured from space is not only highly correlated to human settlement and economic dynamics [6–9], but also provides unique perspectives for revealing environmental and socioeconomic issues [10–13], with great potential for monitoring human activities and understanding related environmental impacts. With a salient advantage over other satellite products from visible, near-infrared, or radar sensors in quantifying the intensity of human activities [14], satellite-based observations of nocturnal lighting have opened up a host of research and application avenues for perceiving the changing world (Figure 1).
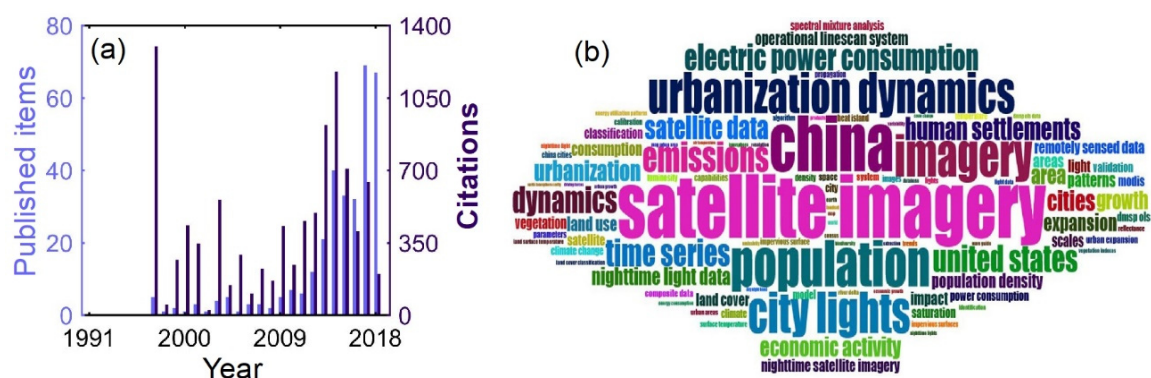
Figure 1. Statistics of satellite-based nighttime light (NTL) publications on (**a**) the published items and citations from 1991 to 2018, and (**b**) the major topics of related publications. The search was conducted using Web of Science with search conditions set as: (TS = (*night-time light* OR *night light* OR *nightlight* OR *nighttime light* OR *light at night* OR *night time light*) AND SU = (Remote Sensing)) AND LANGUAGE: (English) AND DOCUMENT TYPES: (Article). The irrelevant publications retrieved from the search conditions were removed.

Over the past decades, the continuously updated sensors and significantly improved nighttime light (NTL) products and algorithms have been opening opportunities for NTL remote sensing research, which has led to several review papers from different aspects [15–22]. However, current reviews on NTL remote sensing have mainly focused on the widely used NTL products derived from the Defense Meteorological Satellite Program's Operational Line-scan System (DMSP-OLS). Moreover, most of them have focused the applications of NTLs, especially studies on urbanization and socioeconomic activities. A comprehensive review of the current studies using NTL data from different sources, a systematic summary of limitations and challenges of current NTL studies, and some strategies for future NTL studies are still lacking. Meanwhile, the emerging data sources (e.g., geo-located social media data) and techniques (e.g., machine learning/deep learning) also provide additional potentials for broadening and deepening the applications of NTL remote sensing. Understanding and revealing the changes of nighttime lighting observations over time have also started receiving attentions from different fields. Therefore, it is highly needed to systematically re-examine the advances, challenges, and perspectives of NTL remote sensing.

In this paper, we aimed to assess how NTL remote sensing contributes to perceiving human activities and the related environment changes in a changing world. The objective of this paper is

to provide a comprehensive review of satellite remote sensing of NTL observations from datasets to applications, and from challenges to outlooks. The remainder of this paper is organized as follows. In Section 2, we provide an overview of the major NTL datasets. The contribution of nighttime lights (NTLs) to perceiving a changing world is summarized in Section 3, where the major applications of NTL remote sensing are presented. Thereafter, we discuss the challenges and limitations of current NTL applications in Section 4. At the end, we propose the strategic directions for NTL remote sensing research in Section 5.

2. An Overview of Major Nighttime Light Datasets

Given the advances in NTL satellite sensors and technologies, satellite-observed NTLs have emerged as unique geospatial data products that provide a measure of the lighting brightness observed at night from space. This section provides an overview of the major NTL datasets collected from various sensors and platforms (Table 1), including their history and characteristics.

2.1. DMSP-OLS

The earliest DMSP low light imaging system dates back to the 1970s, when DMSP Blocks 5A, B, and C were equipped with the Sensor Aerospace vehicle electronics Package (SAP) instrument from 1970 to 1975. This was followed by the Operational Line System (OLS) sensors, with the first launch in 1976, carried on DMSP Block 5D satellites. From 1990 to 2009, a series of sun-synchronous, polar-orbiting satellites carrying the OLS (i.e. from F10 to F18) were launched to collect NTL images. These data, with 6 bit quantization, were achieved in the form of digital numbers ranging from 0 to 63 in mid-1992, which greatly promoted the accessibility and applications of NTLs, compared to the earlier studies using OLS data on film strips [23]. The follow-on satellites even provided enough overlapping data to allow an inter-calibration between different OLS sensors to overcome the shortcoming of lacking on-board calibration [24].

DMSP-OLS is unique for the presence of a photomultiplier tube (PMT), which intensifies the nighttime visible band signal, allowing the detection of lights from cities, fires, fishing boats, and gas flares, in addition to moonlit clouds. The OLS is an oscillating scan radiometer with a swath width of ~3000 km and consists of two broad spectral bands, a visible near-infrared (VNIR) band (0.4–1.1μm) that collects NTL images, and a thermal infrared (TIR) band (10.5–12.6 μm) [25]. The system has a "fine" spatial resolution mode of 0.56 km and produces "smoothed" data with a nominal spatial resolution of 2.7 km through the on-board averaging of 5 by 5 blocks. With the 14 daily orbits, each DMSP day-night satellite is capable of providing a global nighttime coverage every 24 hours [23]. It can detect the NTL radiance from 1.54×10^{-9} to 3.17×10^{-7} W·cm^{-2}·sr^{-1}·μm^{-1}, and the local overpass time typically varies between approximately 19:30 and 21:30 [26,27].

Currently, three major sets of DMSP-OLS-derived data ranging from daily images to annual composites are commonly used in NTL studies. These data include time series dataset, radiance calibrated dataset, and daily and monthly dataset. These data were developed using a series of improved automatic algorithms by NOAA's National Geophysical Data Center (NGDC) [16,19]. Compared to single daily or monthly images, the annual NTL composites—which are free of charge to general public and less influenced by clouds, fires, lunar illumination, aurora and satellite zenith angle effects—have been mostly used in previous studies [19].

Table 1. The list of major NTL datasets and key features.

Satellite/Sensor	Dataset Type	Accessibility	Available Period	Spatial Resolution	Spectral Bands	Radiometric Resolution
DMSP-OLS	Time series dataset	Free https://www.ngdc.noaa.gov/eog/download.html	1992–2013 Annual	30 arc-second	Panchromatic 400–1100 nm	6 bit
	Radiance calibrated dataset		1996, 1999, 2000, 2003, 2004, 2006, 2010, 2011 Several years			
	Daily and monthly dataset	Not free	Need specially ordered			
Suomi NPP-VIIRS	Monthly VIIRS/DNB composites	Free https://www.ngdc.noaa.gov/eog/download.html	2012.04–present Monthly	15 arc-second	Panchromatic 505–890 nm	14 bit
	Annual VIIRS/DNB composites		2015, 2016 Several years			
	Standard Black Marble product	Free (VNP46A1) https://ladsweb.modaps.eosdis.nasa.gov/	2012.01.19–present Daily	500 m		
	Black Marble High Definition product	Under experiment	N/A	Expected <30 m		
ISS	Astronaut photos onboard ISS	Uncalibrated images free http://eol.jsc.nasa.gov http://www.citiesatnight.org	2003–present Photos taken irregularly	5–200 m	Red, green, and blue (RGB)	8–14 bit
EROS-B	High spatial resolution NTL imagery	Commercial	Mid-2013	0.7 m	Panchromatic	16 bit
JL1-3B	Multi-spectral (red, green, and blue) NTL imagery	Commercial	Launched in 2017	0.92 m	430–512 nm (blue), 489–585 nm (green), and 580–720 nm (red)	8 bit
JL1-07/08	Imagery with a panchromatic band and improved multispectral bands	Commercial	Launched in 2018	/	Panchromatic and multi-spectral (blue, green, red, red edge, and near-infrared bands)	/
LJ1-01	High spatial resolution imagery	Free http://59.175.109.173:8888/app/login.html	Launched in 2018 15-day revisit time	130 m	Panchromatic 480–800 nm	Digital number (DN) values

As the most widely used nighttime dataset, the nighttime stable light (NSL) composites from version 4 time series dataset have experienced several improvements. The earliest global stable light dataset is a geo-referenced composite of nighttime stable light images with a spatial resolution of 1 km, produced using the cloud-free images from 1994 to 1995. This product solely records the percent frequency of cloud-free light detections with no brightness information, which makes it difficult for further research on the intensity of human activities [26]. Subsequently, a global NTL product for the year 2009 was generated using the automatic algorithms for screening the quality of nighttime visible band observations to remove areas with undesirable properties. This product first shows the relative OLS visible band intensities of lit areas, with the ephemeral lighting removed and non-lit areas set to zero [25]. The same methods were then applied to generate the stable NTL composites for the entire digital archive of OLS data. Currently, the latest global annual nighttime stable light composites from 1992 to 2013 can been downloaded from the version 4 DMSP-OLS NTL series on the website of NGDC (https://www.ngdc.noaa.gov/eog/download.html). The time series data include 33 annual composites collected from six different satellites (i.e., F10, F12, F14, F15, F16, and F18) equipped with OLS sensors without an onboard calibration. The annual cloud-free nighttime stable light composites are 30 × 30 arc-seconds gridded nocturnal luminosity spanning the globe from –65 to 75 degrees in latitude. Prior to release of this dataset, related studies mainly used earlier products like the 1994–1995 global stable light dataset and the previous versions of DMSP-OLS NTL series (i.e., Version 1: 1992, 1993, 2000 and Version 2: 1992–2003).

According to the data documentation (https://ngdc.noaa.gov/eog/dmsp/downloadV4composites. html), in addition to the NSL annual composites, the version 4 time series dataset also includes the cloud-free coverages, and the average visible lights and the average lights × percentage. The cloud-free coverage data tally the total number of observations within each 30-arc-second grid cell. This imagery can be used to identify areas with low numbers of observations where the quality is reduced. The average visible data contain the average of visible band digital number values without filtering. The average lights × percentage data is derived from the average visible band digital number (DN) of cloud-free light detections multiplied by the percent frequency of light detection. The inclusion of the percent frequency of detection term normalizes the resulting digital values for variations in the persistence of lighting. These composites are infrequently used in research.

Several radiance-calibrated datasets have been developed to overcome the saturation that occurs in bright urban cores due to the collection of data at high-gain settings. The radiance-calibrated dataset was first developed by Elvidge et al. [23]. Three different fixed-gain settings (i.e., low, medium, and high) obtained from the cloud-free OLS data over 28 nights in 1996 and 1997 were combined in this dataset. This radiance-calibrated data of the United States (US) generated based on the preflight sensor calibration are a major advance over the previous nighttime stable light products [28], allowing for the detection of brightness variations across space in urban cores. However, the coverage of low-light areas is weakened in this dataset. Because of this limitation, a global composite in 2006 was created to capture low brightness levels by blending fixed-gain observations with the nighttime stable light data [29]. The most well-known radiance-calibrated NTL product is the global radiance-calibrated dataset including eight images between 1996 and 2011. This product was collected at varying gains with eight composites inter-calibrated for multitemporal comparison, providing relative radiance values [30]. Though there were no products at different fixed-gain settings from 1992 to 1995 and after 2011, this time series of radiance-calibrated product, with a limited temporal coverage, still provides a unique record of the NTL changes over time without the issue of saturation.

The daily raw images and monthly composites provided by NGDC are mainly used to detect the unstable and short-term light observations for their high temporal resolution compared to the annual composites [31–34]. However, due to the high cost of data acquisition and the complexity of data processing, there are still limited applications using the DMSP-OLS NTL data at the sub-annual timescales.

2.2. NPP-VIIRS

The Visible Infrared Imaging Radiometer Suite (VIIRS) instrument onboard the Suomi National Polar Partnership (NPP) satellite launched in October 2011 was designed to collect high-quality radiometric data [27]. VIIRS, a 22-band visible/infrared sensor, has a same swath width (i.e., 3000 km) as DMSP and a higher spatial resolution (i.e., 375 m and 750 m at nadir). Similar to OLS, VIIRS observes NTLs of the Earth every 24 hours, with the local overpass time after midnight—near 01:30 [27]. Among the 22 bands of VIIRS instrument, the Day/Night Band (DNB) with a spectral range of 0.5–0.9 μm shows an unprecedented capability of night observations [35]. Its three gain settings (i.e., low, mid, and high) allow for detection of a specific dynamic range of approximately 7 orders of magnitude from 3×10^{-9} to 2×10^{-2} W·cm^{-2}·sr^{-1}, with a noise floor at about 5×10^{-11} W·cm^{-2}·sr^{-1} [36–38]. Flown jointly by NASA and NOAA, VIIRS/DNB provides a substantial number of improvements over the DMSP-OLS, including a full in-flight calibration, a higher spatial resolution, a lower detection limit, a wider dynamic range, and a finer radiometric quantization compared to DMSP [27,37,39].

The version 1 suite of VIIRS/DNB cloud-free composites spanning 2012 to present, produced in 15 arc-second geographic grids across the global coverage from 65°S to 75°N, are provided for free by NDGC (https://www.ngdc.noaa.gov/eog/download.html) in a geotiff format with six tiles. Each tile includes both average DNB radiance and the number of corresponding available cloud-free observations. First released in early 2013, the preliminary composites of the version 1 VIIRS product were only generated in moonless nights during two separate time periods: 18–26 April 2012 and 11–23 October 2012 [40]. Subsequently, a series of robust algorithms were developed to exclude low-quality data and extraneous features, followed by an averaging of the light radiance [41,42]. The version 1 nighttime VIIRS/DNB composites include the global monthly NTLs from April 2012 onward. The global annual NTLs in the years of 2015 and 2016 were further processed to remove biomass burning and other extraneous features [42]. Currently, two different configurations of the monthly VIIRS/DNB composites are provided. The "VIIRS cloud mask (vcm)" version, released since April 2012, excludes the data affected by stray light. The "VIIRS cloud mask with stray light (vcmsl)" version, available from January 2014, includes the stray light-corrected data. The second configuration includes the stray light correction described in Mills et al. [41], with a larger spatial coverage toward the poles and a reduced quality. Different from the DMS-stable NTL, the version 1 monthly VIIRS composites record the background noises and ephemeral lights such as biomass burning, aurora and fires. Therefore, attempts [43–46] have been made to correct the VIIRS pixels with unstable NTLs.

The annual composites, produced from the monthly NTLs of the "vcm" version, contain a set of radiance images processed by several filtering steps [42]. In the version 1 suite of annual VIIRS product, four average DNB radiance images are available in each year: (1) "vcm", which is identical to the monthly "vcm" average radiance products; (2) "vcm-ntl", which contains the "vcm" average with the background set to zero; (3) "vcm-orm", which contains cloud-free average radiance values with fires and other ephemeral lights removed; and (4) "vcm-orm-ntl", which contains the "vcm-orm" average with the background set to zero. Additionally, two files for the number of total observations and cloud-free observations are provided. As the latest VIIRS NTL product, the "vcm-orm-ntl" annual version eliminates the effects of ephemeral lights and reduces data outages due to cloud-cover or solar illumination, showing a great advance over the monthly composites [42].

The NASA's standard Black Marble product suite (VNP46), representing the current state-of-the-art NTL data, has been developed to fully explore the potential of the VIIRS time series record. The VNP46 product suite with a spatial resolution of 500 m and a daily-basis processing within 3–5 h after acquisition, providing cloud-free imagery with significant improvements in daily frequency, atmospheric correction, bidirectional reflectance distribution function (BRDF) correction, and seasonal correction, enables both near real-time and long-term monitoring applications [47]. Distributed in Level 3 format, NASA's Black Marble NTL product is available from January 2012 to present using data from VIIRS/DNB aboard the Suomi-NPP satellite. The current Collection V1 VNP46 product suite includes the daily at-sensor top of atmosphere (TOA) nighttime radiance product (VNP46A1), and the daily moonlight-adjusted NTL product (VNP46A2). Multi-source datasets and ancillary data were used to generate high-quality

pixel-based estimates of NTL and corresponding quality flag (QF) information [48,49]. Currently, the VNP46 suite of daily operational products (VNP46A1) is archived and supported by NASA's Level 1 and Atmosphere Archive and Distribution System Distributed Active Archive Center (LAADS DAAC) data center (https://ladsweb.modaps.eosdis.nasa.gov/) in the HDF5 format, whereas the VNP46A2 product is not yet available. The VNP46A1 product contains 26 Science Data Sets (SDS) layers, including sensor radiance, zenith and azimuth angles at sensor, solar, and lunar, cloud mask flag, time, shortwave IR radiance, brightness temperatures, VIIRS quality flags, moon phase angle, and moon illumination fraction, while the VNP46A2 product has six layers containing information on bidirectional reflectance distribution function (BRDF)-corrected NTL (500m), lunar irradiance, mandatory quality flag, latest high-quality retrieval (number of days), snow flag, and cloud mask flag [47]. The VIIRS Black Marble product, with a superior retrieval of NTLs at short time scales and a reduction in background noise, enables quantitative analyses of daily, seasonal, and annual variations of NTLs [48]. Despite a few applications in monitoring electricity supply [50,51] using the preliminary versions of this product, more efforts are needed to explore its great potential in monitoring short-term abrupt changes of NTL and capturing the long-term NTL record, when the standard Black Marble product suite (i.e., Level 3 daily and multi-date formats) is routinely available from the NASA LAADS DAAC.

A description on NASA's Black Marble website (https://viirsland.gsfc.nasa.gov/Products/NASA/BlackMarble.html) reports that the Black Marble high definition (HD) product, a future new suite of higher-level Black Marble product, is being developed by the NASA VIIRS DNB team through the synergistic use of the daily NASA Black Marble standard product with data from other Earth-observing satellites and ancillary data sources. The more detailed information provided by the Black Marble HD product in the near future will potentially enable us to differentiate different types of human activity at the finer scale (<30 m), such as residential, commercial, and industrial sectors. Currently, the monthly Black Marble HD product is experimental.

2.3. Other Satellites and Cubesats

Different from coarse spatial resolution NTLs data from DMSP-OLS and NPP-VIIRS that are widely used for studying human activities and environment changes over large areas, the fine resolution NTL imageries could open up new opportunities in applications of NTL remote sensing. Currently, satellite sensors with a higher capability of NTL detection have already been released or will be released.

One source of such NTL data with fine resolution is photographs taken by astronauts on the International Space Station (ISS). These photos could offer a unique view of the Earth at night in its true colors, and are freely accessible via Gateway to Astronaut Photography of Earth (http://eol.jsc.nasa.gov). To address the difficulty in finding an ISS image of a specific city among millions of images, the atlas of astronaut photos of Earth at night [52] was developed to allow easy access to the images (http://www.citiesatnight.org). Although the astronaut photos can reflect more details of the Earth with a spatial resolution from 5 to 200 m [53], technical challenges in radiometric calibration and unevenly temporal and spatial distributions of these original photos hinder the wide application of ISS images. Based on a collaboration between the Complutense University of Madrid, NASA, and ESA, the calibrated ISS images became available through paid service at NOKTOsat (https://www.noktosat.com/). Currently, the ISS images have been used for studies on identification of urban and internal lighting types [54–57], light pollution [58,59], and socioeconomic activities [60–62].

The first source of high spatial resolution NTL imagery from space was from the commercial satellite of EROS-B, which started providing fine spatial resolution observations of NTLs (i.e., 0.7 m) in 2013 with a spectral band wavelength range of 0.5–0.9 μm and a dynamic range of 10 bits. It opened new avenues for studying the spatial pattern and light pollution of artificial lights in cities worldwide [63]. However, as the NTL images of EROS-B are panchromatic, the lighting type cannot be identified from this data [63].

Another commercial satellite with a high spatial resolution is JL1-3B from China. Launched in 2017, this satellite enables multi-spectral (red, green, and blue) NTL imageries at a spatial resolution of 0.92 m with a capability to detect light as low as $7E–7$ $W \cdot cm^{-2} \cdot sr^{-1}$ [64]. With advantages of the

fine-resolution details and multispectral information, as well as its on-board radiance calibration, new capabilities of lighting types and nightscape patterns are promising in future studies. Additionally, the next-generation of JL1-07/08 satellite launched in 2018 has both a panchromatic band and improved multispectral bands (i.e., blue, green, red, red edge, and near-infrared), and brings possibility for a better understanding of NTLs on environmental impacts, such as the impact of powerful lights on nocturnal bird migration [65].

Different from other commercial NTL satellites, cubesat has the potential of providing valuable data at a relatively lower cost [66]. An example of a recent cubesat is LJ1-01, which was launched in 2018. This is a 20 kg-level micro-nano satellite equipped with a high-sensitivity night-light camera that has a spectral bandwidth of 0.319 μm. It offers a global high-precision NTL observation with a dynamic range up to 14 bits at night. The LJ1-01 imageries, with a spatial resolution of 130 m and a swath of 250 km, are free to download at the High-Resolution Earth Observation System of the Hubei Data and Application Center (http://59.175.109.173:8888/app/login.html). The LJ1-01 data are well-correlated to the VIIRS images, but provide more spatial details and show better capability of change detection [67]. However, the current lack of multi-temporal images and the effects of clouds and moonlight limit its widespread application [68,69]. Differently, the existing visible wavelength cameras on AeroCube satellites (e.g., AC-4 and AC-5) can provide multi-color night lights [70].

3. Contributions of Nighttime Lights to Perceiving the Changing World

Through a host of novel applications, NTL remote sensing deepens our understanding of the influence of human activity on the increasingly-threatened environment of the Earth surface (Figure 2). In this section, we summarize the major contributions of satellite-based NTLs to perceiving the changing world from two dimensions: Human activities and environmental changes.
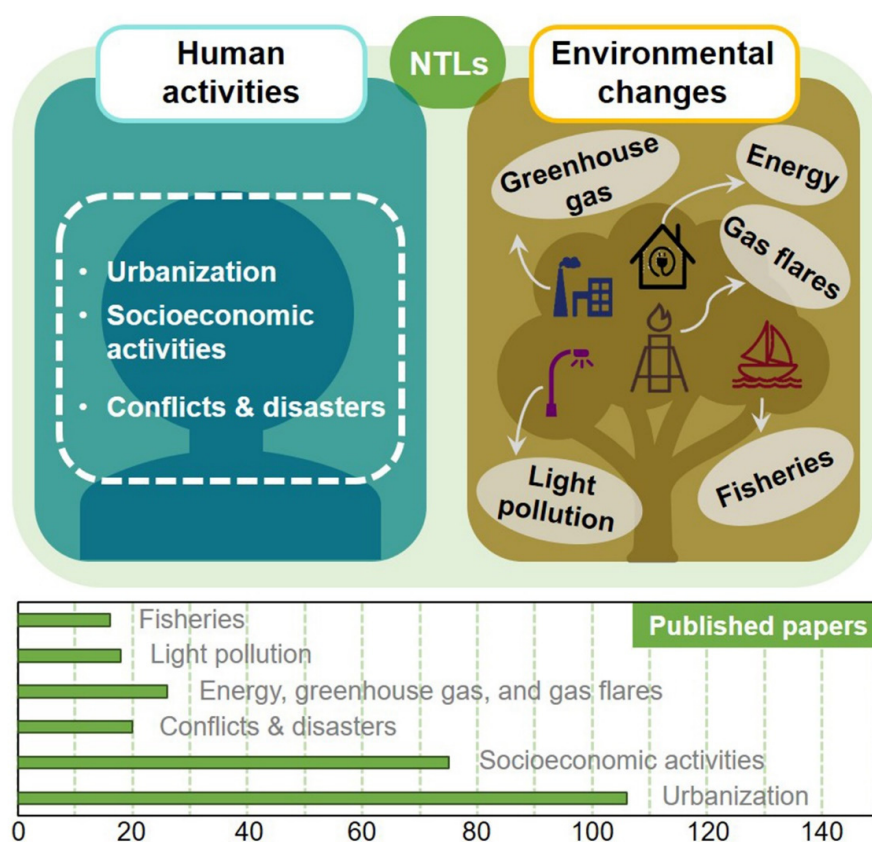
Figure 2. Applications of satellite-based NTL remote sensing for perceiving the changing world from two dimensions: Human activities and environmental changes. Published papers of different topics were derived from results in Figure 1a.

3.1. Human Activities

3.1.1. Urbanization

NTL data have been extensively used in urban mapping from global to local scales (Table 1). More than five global products have been developed from NTL data. In the first dataset, the global urban area in 2000 was mapped using the DMSP-OLS NTL data and an optimized threshold method [71,72]. In the second dataset, NPP-VIIRS NTL data and MODIS multispectral data were combined to map urban areas using the enhanced urban built-up index [73]. In the third dataset, a full convolutional network was used to classify urban areas from 1992 to 2016 using both NPP-VIIRS and DMSP-OLS NTL data, as well as the normalized difference vegetation index (NDVI) and land surface temperature (LST) data from AVHRR and MODIS [74]. In the fourth dataset, a series of spatially and temporally consistent global urban maps from 1992 to 2013 were developed using a quantile-based approach and DMSP-OLS NTL data [75]. In the fifth dataset, the global urban areas from 2000 to 2012 were mapped by applying a region-growing support vector machine classifier and a bidirectional Markov random field model [76]. There are also several datasets of urban areas at national and regional scales using NTL data (Table 2). The "hotspots" of mapping urban areas at the national and regional scales include China and USA.

NTL data have been used to map impervious surface area from urban areas. Originally, NTL data were mostly used to map urban areas, which are defined as the areas dominated by artificial surfaces [77]. Various terms have been used to represent urban areas, such as built-up area [78,79], urban extent [80,81], and urban boundary [82,83]. The extent of impervious surfaces is smaller than the extent of urban areas because an impervious surface is artificial surface that water cannot penetrate, including rooftops, paved roads, and parking lots [77]. In previous studies, regression-based methods have been used to capture the relationship between NTL data and impervious surface area. For example, Sutton et al. [84] used a multivariate linear regression method to estimate impervious surfaces in the US based on NTL data and population grid data. Ma et al. [85] also used a linear regression method to map impervious surfaces in China using NTL and NDVI data.

The methods for mapping urban areas can be grouped into three major categories. The first category is the threshold-based method. This method was originally proposed by Imhoff et al. [86] to map urban areas in the US using a single threshold. However, the threshold can vary among regions and over time [82]. Therefore, researchers adopted multiple thresholds among regions [87], and used segmentation-based methods to identity local-optimized thresholds [71,80]. The second category is based on the supervised classification. Representative methods vary from the traditional K-nearest-neighbors classification, to complex machine learning and deep learning methods, for example, support vector machine [88], random forest [89], and fully convolutional network [74]. In the third category, the statistic relationship between indices derived from NTL data, such as the enhanced urban built-up index [73] and the human settlement index [78,90], and observations of urban area has been proposed to estimate urban areas.

Ancillary data have also been widely integrated to enhance the mapping ability of NTL data. The datasets of NDVI and LST have commonly been used as ancillary data for this purpose. Specifically, NDVI can be used to differentiate bare soil and water surface from urban land, which is difficult to separate as NTL data have a saturation issue. LST data can be further used to separate urban area from vegetation cover because urban heat island effect caused by impervious surfaces could increase LST in urban areas, and the irrigated vegetation cover within cities in semi-arid and arid regions could decrease LST in non-urban areas [91].

Table 2. Representative products of urban areas from NTL data.

Object	Scale	Nighttime Light Data	Ancillary Data	Time	Method	Reference
Urban area (built-up area)	Global	DMSP/OLS		2000	Cluster-based method + thresholds	(Zhou et al., 2014; 2015)
		VIIRS/NPP	MODIS multispectral data	2014	Enhanced urban built-up index	(Sharma et al., 2016)
		VIIRS/NPP + DMSP/OLS	NDVI, LST	1992–2016	Fully convolutional network	(He et al., 2019)
		DMSP/OLS		1992–2013	Quantile-based approach	(Zhou et al., 2018)
		DMSP/OLS	MODIS NDVI MODIS LST	2000–2012	Support vector machine classifier and Markov random field model	(Chen et al., 2019)
	National	DMSP/OLS		1992–2008	Iterative unsupervised classification method	(Zhang and Seto, 2011)
		DMSP/OLS		1992–2008	Regional thresholds	(Liu et al., 2012)
		DMSP/OLS		1994–1995	A global threshold	(Imhoff et al., 1997)
		DMSP/OLS		2005, 2010	Object-based urban thresholding	(Xie and Weng, 2016)
		VIIRS/NPP		2015	Multiple methods	(Dou et al., 2017)
	Regional and city	DMSP/OLS		1994–1995 1996–1997	Threshold	(Henderson et al., 2003)
		DMSP/OLS	SPOT NDVI	2000	Support vector machine-based region growing algorithm	(Cao et al., 2009)
		DMSP/OLS	MODIS NDVI	2001–2007	Human settlement index	(Roychowdhury and Maithani, 2010)
		VIIRS/NPP		2012	Regional thresholds	(Shi et al., 2014)
Impervious surfaces	National	DMSP/OLS	Population distribution	2000–2001	Multivariate linear regression	(Sutton et al., 2009)
		DMSP/OLS	AVHRR NDVI	1992–2009	Vegetation adjusted nighttime light urban index and linear regression	(Ma et al., 2014).

3.1.2. Socioeconomic Activities

Remotely-sensed anthropogenic lighting signals and their spatial variations at night provide us with an efficient proxy measure of the demographic and economic related activities during urbanization and regional development. Hence, satellite-derived NTL data, especially the long-term archive data collected by the DMSP-OLS and the observations of NTLs from NPP-VIIRS, have been widely used to estimate population [92,93], GDP [44,94], and other economic statistics such as income [95], copper stock [96], and freight traffic [97]. However, the quantitative relationship between NTL signals and statistical variables varies with both time and space. These variations make it difficult to further clarify the quantitative responses of NTL signals to corresponding socioeconomic activities. For example, Zhu et al. [98] showed that the best-fitting model could be the power function model, quadratic polynomial model, or the linear model, when modeling the GDP dynamics in different provinces/years in China. This variation of statistical relationship between NTLs and socioeconomic activities depends on either the real background of land surface or the local status, showing different responses in urbanized areas and rural areas, or in regions with diverse land use types or industry distributions. Therefore, the ancillary data, such as geo-spatial data, regional background, and status, are needed to improve the accuracy of estimation of socioeconomic parameters [99].

The current studies for assessing socioeconomic activities using NTL remote sensing can be grouped into four categories: (1) Investigating socioeconomic status at finer spatial scales [7,44,100]; (2) tracking socioeconomic dynamics at higher temporal frequency [101]; (3) quantifying socioeconomic parameters for data-missing areas [102]; and (4) evaluating development levels to reveal geographical phenomena and social issues, such as regional inequality [5,103,104], ghost town [11,105], and poverty [10,106–108]. Disaggregating the socioeconomic variables from the administrative unit into grids not only provides a detailed detection of demographic and economic dynamics at finer spatiotemporal scales than official statistics, but can also help further explain their changes and investigate the issues behind these changes. By use of the global radiance-calibrated NTL data, Henderson et al. [109] explored the distribution of economic activities using two groups of characteristics (i.e., agriculture and trade), indicating that the agriculture variables show a relatively higher explanatory power in early developed countries and that the trade variables are more important in lately developed countries, despite the fact that the latter group of countries are more dependent on agriculture. Zhao et al. [44] found that the long-term observations of economic differences at diverse geomorphological types is of great significance for regional sustainable development, considering the impact of terrain conditions (e.g., elevation and relief) on industrial layout and urban planning.

New NTL data and improved methods and models open new avenues for socioeconomic studies using NTL remote sensing. The new generation of NTL data collected by NPP-VIIRS has proved to be more indicative of economic activities than DMSP-OLS at the regional and local scales [45,46,110], and therefore has enabled the mapping of socioeconomic parameters from coarse resolutions (5 km, 1 km) to finer resolution (0.5 km) [44,100,111]. Moreover, the spatial connection between NTL signals and land surface types at fine scales [112,113], which is crucially important for further socioeconomic applications of NTL data, has started getting attentions. In addition to widely used official statistics [44,94] and remotely-sensed thematic products such as land cover data and population map [103,112,114], the increasingly popular geo-located big data, closely related to population dynamics, has started being used to explore the association between NTL signals and corresponding human activities, particularly at fine spatiotemporal scales [115].

3.1.3. Conflicts and Disasters

While the increase of NTL brightness is always related to economic growth and urbanization, its decrease can be caused by conflicts and natural disasters. One pioneering study, using 159 countries as samples, shows that the NTL fluctuation, measured by an NTL variation index, is correlated to armed conflicts, with higher fluctuations indicating higher probability of occurrence of armed conflicts [116]. The Syrian Civil War occurred in 2011. Although there are massive media reports, getting a whole picture

of the war is challenging work. By using 38 monthly composites of DMSP-OLS, the spatiotemporal patterns of NTL in Syria have been revealed, showing that the number of refugees is positively correlated to NTL loss, suggesting that satellite-observed nighttime light is a good indicator of the humanitarian crisis in Syria [117]. Although DMSP-OLS is an effective indicator of the Syrian Civil War, NOAA stopped producing DMSP-OLS composites from February 2014, with VIIRS monthly composites as the substitution. By inter-calibrating DMSP-OLS and VIIRS monthly composites, the NTL dynamics during January 2011 to January 2017 were analyzed, showing a slight recovery of NTL due to the peace agreement between the Syrian Government and the rebel groups [118]. In addition to the Syrian conflict, VIIRS images have also been applied to analyze the civil wars in Yemen [119] and Iraq [120,121], showing that the time series VIIRS images are able to reflect electricity usage during the war.

Similar to conflicts, natural disasters, such as tsunamis, hurricanes, and earthquakes, can also have sudden but severe impacts on NTLs, providing an opportunity to evaluate the damage of these disasters. In December 2004, a tsunami that was triggered by a 9.2 magnitude earthquake attacked Northern Sumatra, Indonesia, killing about 160,000 persons. Time series of annual DMSP-OLS images were used to calculate the NTL change in this region, showing a significant drop of NTL after the tsunami and a partial recovery of NTL after the reconstruction, and these results are highly consistent to the house survey results [122]. Based on econometric models, economists were able to assess the economic loss after typhoons in China using time series of annual DMSP-OLS images and historical typhoon track data. It was found that there was a net loss of $28.34 billion in China due to typhoons between 1992 and 2010 [123]. As disasters are processes compressed in time [124], the fine temporal resolution of NTL data are of significance for a timely assessment of abrupt changes in power delivery caused by disasters such as storms, earthquakes, and floods. Compared to the DMSP-OLS annual composites, which are able to measure the long-term economic change due to the disasters, VIIRS daily images can capture more details of disasters in temporal dimension. VIIRS daily images have been used to compare the light before and after two storms in Washington D.C., showing that the daily data have a clear response to the power outage resulted from the storms [125]. In addition, a more comprehensive study, focusing on earthquakes, floods, and storms, shows that the time series of VIIRS images are useful to detect the power outage from these disasters, but the cloud is a major limitation of the detection ability [126]. While the VIIRS daily product is a potentially good tool to monitor conflicts and natural disasters, images are affected by a number of factors including moonlight and atmospheric conditions, as well as the clouds. Additionally, the NASA Black Marble NTL data, a new type of high-quality NTL derived from NPP-VIIRS DNB, have started to be applied to disaster monitoring to estimate disaster-related power outages [50] and construct high-resolution maps of electrical grid restoration [51]. These preliminary results demonstrate that Black Marble NTL data can serves as good data source to detect the abrupt changes of power delivery caused by disasters or conflicts.

3.2. Environmental Changes

3.2.1. Fisheries

NTL data are effective in detecting fishery information, because it is common to install high-power bulbs on fishing boats to attract phototaxis species (e.g., squid and sardine). The earliest publication noting this capability of NTL is dated back to the late 1970s [127]. DMSP-OLS images have been widely used to detect the spatial and temporal variability of fishing vessel lights in the Sea of Japan [128,129], Southwest Atlantic [130,131], and Peru [31,132]. These studies estimated the illuminated area by calibrating monthly DMSP-OLS images using the ship location data from local surveys, so that the fishing extent, intensity, and recurrence could be quantified.

However, the application of DMSP-OLS imagery has been limited due to the lack of an automatic algorithm for detecting boats using NTLs. Such an issue could be addressed by using VIIRS/DNB data, owning to its better capability for detecting lit fishing boat features compared to DMSP data [133]. The Earth Observation Group (EOG) developed a boat detection algorithm for VIIRS data in 2014 [133].

Currently, VIIRS boat detection (VBD), a global product with nominal 4 h temporal latency, is widely used by fishery agencies in Asia. The nightly VBD archive extends back to April 2012, and monthly and annual summary grids have also been produced by EOG. This opens up the opportunity to use the near real-time VBD to estimate fish stocks [134,135], rate the compliance levels of fishery closures [136], and identify illegal fishing [137–139]. The fishery information derived from VBD data can aid international efforts toward sustainable fisheries and marine conversation. A recent study on the cross-matching of VBD with vessel monitoring system (VMS) data in Indonesia revealed the fishing gear types and found that VIIRS detects nine times more vessels than the VMS tracks [140].

3.2.2. Energy, Greenhouse Gas, and Gas Flares

NTL data provide an effective proxy for estimating energy consumption and green gas emissions [111,141]. With accelerated urbanization and industrialization since the Industrial Revolution, energy consumption such as electric power consumption (EPC) has been rapidly increasing, leading to a large amount of emissions of greenhouse gas, such as carbon dioxide (CO_2) emissions [142,143]. Estimating the spatiotemporal dynamics of energy consumption and green gas emissions has significant implications for local authorities to guide their policies in carbon reduction and climate change. In the mid-1990s, Elvidge et al. [144] and Doll et al. [111] firstly found a strong relationship between DMSP-OLS data and EPC and total CO_2 emissions, respectively. Shi et al. [145] revealed that the NPP-VIIRS data could be a more powerful tool for modeling EPC and other energy consumption-related indicators. As the spatial distribution of EPC and CO_2 emissions was not specifically represented in early studies [144,146], more attempts were then made to map the spatiotemporal dynamics of EPC and CO_2 emissions using NTL data [147–149]. For example, NTL data have been extensively used to estimate EPC and CO_2 emissions at multi-scales [46,141,150,151] and in a long time series [152,153]. Although NTL data did a superb job in revealing the spatiotemporal distribution of EPC and CO_2 emissions, these studies vary regarding the studied source of CO_2 emissions using NTL data. Some studies focused on CO_2 emissions from electric power consumption [144,154,155], while other studies investigated CO_2 emissions from fossil fuel combustion [148,156–158] or residential energy consumption [159].

In the last decades, studies of electric power consumption and CO_2 emissions using NTL data can be divided into three classes: (1) Mapping the spatial distribution of EPC and CO_2 emissions from urban to global scales [160–162]; (2) exploring spatiotemporal dynamics of EPC and CO_2 emissions using time-series NTL data [153,163,164]; and (3) improving the accuracy of EPC and CO_2 estimation with the consideration of saturation and unlit areas [144,156].

Mapping the spatial distribution of EPC and CO_2 emissions at the global, national, regional, and even urban scales using NTL data has received increasing attention in the context of global warming. These efforts have improved our understanding of energy consumption and green gas emissions from the spatial dimension, showing a great a potential for further analysis when integrated with other geo-spatial data [153]. Using the cloud-free radiance-calibrated DMSP-OLS nighttime images, Lo [160] established the logarithmic relationship between EPC and lit area for 35 Chinese capital cities. Amaral et al. [141] estimated EPC in the Brazilian Amazon from extracted lit area at the municipal level by inter-calibrating the global NSL data via a modified invariant region (MIR) method. For the spatial distribution of CO_2, a global 1×1 km annual CO_2 emissions inventory was developed using NTL data [147]. By combining NTL data with statistical data at administrative levels, urban CO_2 emissions across multiple spatial scales in China were assessed to further discuss the variations of CO_2 emissions among different geographic regions [165]. Su et al. [166] not only estimated CO_2 emissions data of China at the finer city scales, but also analyzed the driving factors and proposed corresponding mitigation recommendations. Shi et al. [167] investigated spatial variations of CO_2 emissions and their impact factors across different levels, and offered evidences for CO_2 emissions mitigation policy making. These studies using NTL data have promoted the spatial estimation of EPC and CO_2 emissions because of the limitations in the statistical data, such as the inconsistency in these data at different administrative levels and the lack of enough data at city or local levels.

The availability of time series NTL data makes it possible to monitor the spatiotemporal dynamics of EPC and CO_2 emissions for a better understanding of energy consumption and green gas emissions. These time series composites include three types: DMSP nighttime stable light data, DMSP radiance-calibrated NTL data, and VIIRS monthly NTL data. He et al. [163] mapped electricity consumption at the county level of China during 1995–2008. Shi et al. [153] detected spatiotemporal dynamics of global EPC from 1992 to 2013, and latterly they explored spatiotemporal patterns of EPC in countries along the Belt and Road. Results demonstrate that EPC growth mainly occurred in the developing countries, and GDP is a more important impact factor for EPC compared to population [168]. Lately, Shi et al. [169] evaluated the spatiotemporal patterns of urban EPC within different spatial boundaries (i.e., the city administrative area, city district, urban center, and urban built-up area) from 1992 to 2013. Despite the annual NPP-VIIRS data having a higher spatial resolution, more efforts are needed to remove the background noise before monitoring EPC and CO_2 emissions [158]. Considering the short time series of NPP-VIIRS data, DMSP-OLS data are still the main NTL dataset for analyzing the spatiotemporal dynamics of EPC and CO_2 emissions [145].

As the inherent limitations of NTL data greatly affect the estimated EPC and CO_2 emissions, numerous studies have been conducted to improve the accuracy of EPC and CO_2 estimations. First, more attentions have been paid when monitoring EPC and CO_2 emissions in urban areas where the NTL brightness is saturated. Various methods have been proposed to improve saturated pixels in the NTL imagery; for instance, modifying DMSP-OLS NTL data by using an Enhanced Vegetation Index (EVI) [162]. A delta model was proposed to restore the saturated pixels at the center of a light patch [170] by developing a cubic regression method [171]. In addition, the integration of NTLs with other data, such as population data [148,156] and the vegetable index [172], was proved to help improve the accuracy of spatiotemporal distributions of EPC. Second, the estimation of EPC and CO_2 emissions in unlit areas is still a challenge. The ratio of estimated emissions in unlit area to lit area greatly affects the accuracy of the estimation. For instance, Meng et al. [173] adopted a ratio of 0.38 for emissions per capita in unlit area to lit area, while Ghosh et al. [148] used a ratio of 0.5 when spatializing the CO_2 emissions using other data (e.g., LandScan population density).

NTL data also show great potentials in capturing gas flaring activities over large areas [174], due to specific characteristics that are easily distinguished from city lights at night [26]. Although gas flaring is a widely used practice to dispose of associated gas from oil production and processing, its spatiotemporal pattern is difficult to obtain before the emergence of NTL data [175]. NPP-VIIRS data, with a unique ability in collecting near-infrared and short-wave infrared (SWIR) data at night, is extremely useful for detecting flares and measuring their radiant output [175]. It is worth noting that gas flares may introduce uncertainties in estimating CO_2 emissions [176]. A study commissioned and funded by the World Bank's Global Gas Flaring Reduction partnership [174] estimated national and global gas flaring volumes using NTL data across a series of years and provided a time series of global gas flares maps. This work greatly contributes to reducing the impact of gas flares on mapping urbanization and carbon emissions.

3.2.3. Light Pollution and Associated Effects

NTL data have provided unique data to study the environmental and ecological effects of artificial lights with extensive spatial and temporal coverages. Although the wide use of artificial light at night has brought significant convenience to humankind, the dramatic change of the NTL environment inevitably affects both the ecosystem and human life, known as "light pollution" [177]. NTL data have brought new opportunities for light pollution studies, enabling evaluation over large areas with low costs compared to the traditional ground-based observations and laboratory studies [178,179]. Currently, studies of light pollution based on satellite-derived NTL data mainly lie in three aspects: (1) Characterizing and surveying the distribution of light pollution; (2) revealing the impacts of NTLs on ecological environment and species; and (3) estimating the impact on human health brought by artificial light at night.

Widespread studies have been conducted to characterize the distribution of light pollution from local [68,180–182], national [183–185], regional [186], and global scales [187,188] using various NTL datasets derived from different sensors. The distribution of light pollution in both developed areas, such as Europe [181,182,186], and fast developing areas, such as China [13,68,179,183,184] and Pakistan [185], have been investigated using the time series of NTL data from the DMSP-OLS. Necessary data preprocessing has been performed for consistent and comparable light pollution mapping. Quantitative indicators such as total nighttime light (TNL), night light mean (NTM), and night light standard deviation (NTSD) were proposed to capture trends of light pollution [184]. The levels of light pollution change were also used to map the changing patterns [13]. Compared to NTLs with coarser resolutions such as stable NTLs and calibrated NTLs, the finer resolution NTL images from VIIRS, EROS-B, and Luojia 1-01 and ISS, have shown great potentials for investigating spatial patterns of artificial light pollution [53,67,68,178,189].

NTL data also provide a convenient way for evaluating the impact of light pollution on the ecological environment and species. Trends and patterns of light pollutions were assessed for various ecosystems [190], vegetation [191], and habitat types [192] to investigate the degree of exposure to light pollutions. It was found that the threat of light pollution to the global biodiversity was emerging, especially in areas with high biodiversity [192]. As a good indicator, NTL data have also been used to measure the conservation efficiency of protected areas [13,179,193,194], because there is low or even no light pollution in a well-protected area. Additionally, the behavior and presence of some species, such as marine turtles and nocturnally-migrating birds, were also studied using NTL remote sensing technology, because of their sensitive responses to artificial light at night [58]. The impact of light pollution on marine turtles has been extensively investigated, including: (1) Examining temporal changes in artificial lighting at marine turtle nesting areas and identifying the nesting sites with the greatest threat from artificial light [12,195]; (2) investigating the relationship between the long-term spatial patterns of sea turtles and the corresponding NTL intensity for explaining sea turtle nesting activities [58]; and (3) analyzing the difference of the relationship between sea turtle activities and NTL intensity among different sea turtle species [189]. Similar methods have been used to study the impacts of light pollution on nocturnally-migrating birds [196,197], revealing that urban sources of artificial light at night can broadly affect the migratory behavior of nocturnally-migrating birds.

NTL data have been also used to study the effect of light pollution on human health. These studies, carried out in different regions and population cohorts, provided mutually complementing evidence about the significant association between artificial light at night and a variety of adverse health phenomena, such as breast cancer [198–202] and obesity [203,204]. Moreover, a stronger association between artificial light at night and breast cancer incidence was found using VIIRS/DNB images with a finer spatial resolution compared to DMSP data [204]. Studies using images with higher resolution and multi-spectral bands taken from the ISS demonstrated that exposure to the blue-light spectrum of outdoor artificial light at night appeared to have stronger effects on hormone-dependent cancer incidence (i.e., prostate and breast cancers) compared to the green-light and red-light spectrums [205,206]. Using VIIRS/DNB images and ISS photos of outdoor light, a comparison of personal measurements with satellite-based estimates of exposure to night light found a discrepancy between outdoor NTL and indoor light exposure [207], indicating that the modifying factors should be used when using the satellite NTL to evaluate potential effects of night light on human health. Such findings can help make better policies for minimizing the adverse health effects of artificial light exposure on human health. Related studies will benefit from improvements of NTL images in spatial resolutions and spectral information.

4. Challenges and Limitations of Current Nighttime Light Studies

Despite of the widespread use of NTL images for perceiving the changing world, challenges still exist in current NTL applications due to limitations from both data and methods (Figure 3). These challenges and limitations are summarized below.
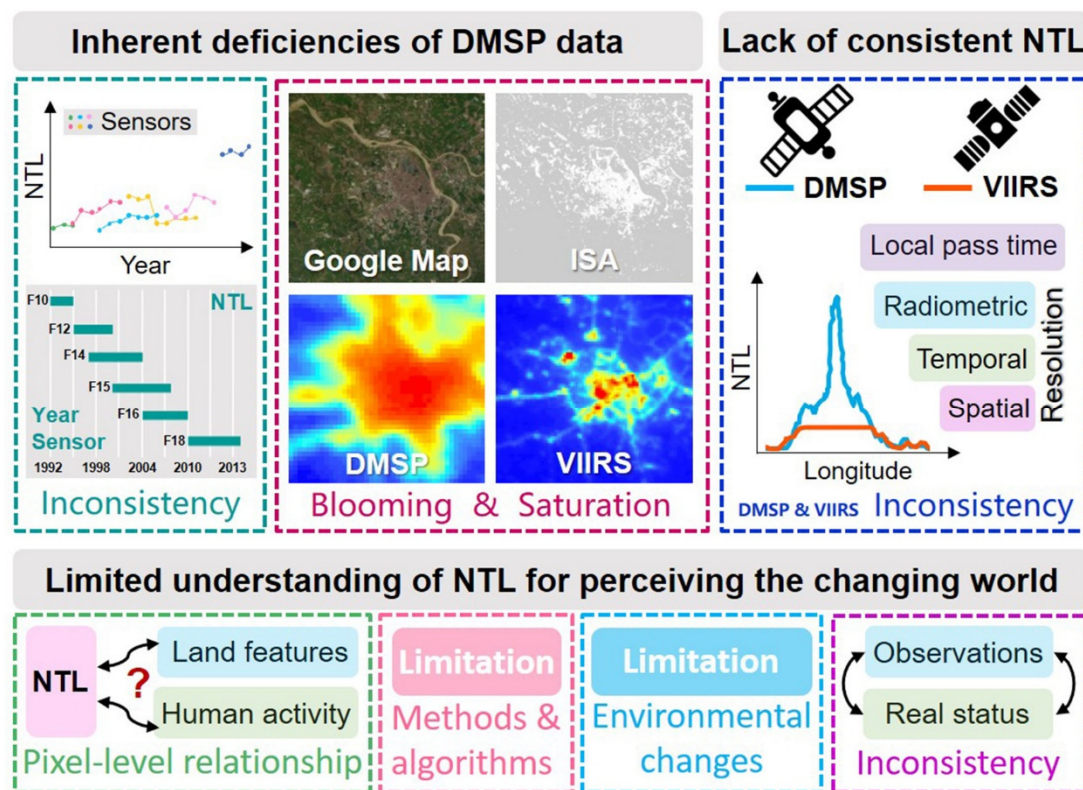
Figure 3. A schematic of challenges and limitations in current NTL studies.

4.1. Inherent Deficiencies of the Long Time Series of DMSP Data

4.1.1. Inconsistency Among Different DMSP Sensors

The time series of DMSP NTL data cannot be directly compared for dynamics across years due to the lack of on-board calibration, varied atmospheric conditions, and satellite shift and sensor degradation [24]. The DMSP NTL time series data consists of observations from six satellites during the period of 1992–2013, namely, F10 (1992–1994), F12 (1994–1999), F14 (1997–2003), F15 (2000–2007), F16 (2004–2009), and F18 (2010–2013). Because of the systematic differences in satellite orbits (i.e., dawn pass versus dusk pass) and sensor degradation, the collected NTL data from different satellites are notably different. In addition, without on-board calibration, the NTL observations derived from the same satellite are different across years due to different atmospheric conditions. The temporal inconsistency of DMSP NTL time series data considerably limits its applications for dynamic studies such as urban expansion and electricity consumption.

Existing studies on addressing the temporal inconsistency of DMSP data have focused on inter-calibration of NTL time series data, using empirical relationships between the calibrated and referred images. Due to the lack of established calibration sites for DMSP-OLS [208], such relationships were built by manually selecting stable regions as references [87,175,186,209,210] or automatically identifying stable pixels as pseudo-invariant features [208,211]. Elvidge et al. [174] proposed a general framework for DMSP NTL inter-calibration by identifying a reference region that is relatively stable across years, but meanwhile contains different DN values. This calibration paradigm has been widely used in subsequent studies [87,186,209,210], in which different empirical models and regression parameters obtained from different reference regions were used for inter-calibration at the local or global scale. Later, improved approaches [208,211] using globally and regionally consistent bias to collect stable DN pixels were proposed for NTL inter-calibration, without the need of selecting calibration sites from one or more locations. Differently, Li and Zhou [24] developed a stepwise calibration strategy to adjust NTL images from different satellites in a systematic manner. The derived results are temporally

consistent at the global scale in terms of the total lit pixels and the NTL luminance. There are also a few studies in which the radiance calibration of DMSP was conducted using the ground-based light sources [212]. However, these approaches are more suitable for local-area studies due to the limited data from field measurements.

Although these studies used different approaches for inter-calibration of DMSP NTL data, the empirical relationship between the calibrated and referred observations is the key to addressing the temporal inconsistency of DMSP data. Such a relationship is sensitive to the selected reference image, including the selected regions/pixels and year/satellite, and the adopted models, making the derived result different across different studies [213]. One exception is a study by Li and Zhou [24] that is different from most previous studies, in which a notable modification of the TNL range was likely to be observed because only one reference image was used to calibrate the entire time series. Calibration with large modifications may affect the reliability of acquiring useful information from NTL images. Despite that inter-calibration methods have greatly improved the inconsistency observed in raw NTL time series generated from aggregating lit pixels over a region, the inconsistency in raw NTL time series at the pixel level is observed to be only moderately improved [213].

4.1.2. Saturation and Blooming Effects of DMSP Data

The DMSP NTL data have two major deficiencies: The saturation effect of DN values in urban cores and the blooming effect in suburban and rural transition areas. On the one hand, due to the collection of DMSP data at high gain settings, regions with high luminance might show the same DN values (i.e., DN = 63) as areas with relatively lower luminance, making it difficult to differentiate the highly-lit pixels. Such a deficiency may limit applications of DMSP NTL data in studies of urban environment change such as light pollution. Also, the saturated DN of NTL data in urban cores would lead to an underestimation of socioeconomic activities, such as electricity consumption in said urban cores. On the other hand, because of the blooming effect in DMSP NTL data, a notable overestimation of luminance over suburban and surrounding rural areas has been found, which challenges applications of NTL data such as urban extent mapping. Also, the bloomed lit pixels with biased luminance have notable impacts on relevant socioeconomic studies (e.g., population and GDP) using DMSP NTL data.

Incorporating land surface features and demographic information is a commonly used approach to mitigate the saturation effect of DMSP NTL data, resulting in modified NTL indices. NDVI is a widely used indicator to reduce saturation and increase variations to generate modified NTL indices [214]. Similarly, other indicators such as normalized difference water index (NDWI) [215] and urban fraction data can also be used to modify NTL indices [71]. In addition to land surface features, demographic information is also helpful to reduce the saturation effect of NTL pixels. Spatially-explicit population density data has been introduced to enhance the heterogeneity of saturated NTL pixels [93]. In addition, socio-media data, such as volunteered data and mobile-based check-in data, are new data sources of human activities to address the saturation of DMSP NTL data [216]. The key of these approaches is to generate heterogeneous modified NTL indices in high-luminance areas, and these modified NTL indices show improved performances in investigating human activities in urban core areas compared to raw DN values.

The threshold-based approach and classification are two widely used approaches to address the blooming effect in studies such as NTL-based urban extent mapping. The threshold is used to separate urban from surrounding suburban and rural areas. However, the thresholds vary in different regions due to different socioeconomic development levels. Zhou et al. [71] applied the estimated optimal threshold for each potential urban cluster with different sizes, using a cluster-based approach. Ancillary information such as statistical urban areas from survey data [8] and fine-resolution land cover data [72,217] are widely used when determining the optimal threshold. Recently, a quantile-based approach according to the gradient change of NTL luminance was developed to automatically derive the optimal threshold to delineate urban extent [75]. This approach can maximally separate urban from surrounding rural areas based on the DN distribution of NTL data, and it is extendable both in

space and in time. Classification is an alternative approach to derive urban extents using NTL data, where other support information such as NDVI is required [88].

4.2. Lack of a Long Time Series of Consistent Nighttime Light Observations

Two major NTL datasets (i.e., DMSP and VIIRS) have been widely used in previous studies. One is the version 4 DMSP stable NTL product (1992–2013), and the other is the version 1 suite of VIIRS monthly NTL composites (2012 to date). Compared to DMSP-OLS stable cloud-free composites, NPP-VIIRS imageries have a finer spatial resolution, a wider dynamic range, and a higher radiometric resolution, which provide a clearer and more detailed snapshot of anthropogenic light emissions at night [218]. An onboard calibration was also used to enhance the quality of NPP-VIIRS data. With improvements in the spatial resolution, consistency, dynamic range, and radiometric quantization, the issues of saturation effects in urban cores and blooming issues are not significant as DMSP-OLS [27,219] and NPP-VIIRS data can be used directly for temporal analyses. Moreover, the difference in the overpass time of these two sensors also causes inconsistency of the detected lighting in the two datasets [27], because the nightscape dynamics are different over time from the early evening to midnight [53,220]. This inconsistency is obvious in large cities and in areas where the streetlights intentionally become dim or turn off at late hours.

The differences between DMSP-OLS and NPP-VIIRS have led to related studies for a better understanding of these two datasets and their differences. In a number of studies, the capability of NPP-VIIRS and DMSP-OLS have been compared in analyzing urbanization [79,221], socioeconomic activities [43,45,145,222], greenhouse gas emissions [158,223], and light pollution and its effects [204]. These attempts, which have emphasized the advantages of VIIRS data in detecting human activities at fine scales, have promoted new and improved methods to overcome the inherent deficiencies of DMSP data mentioned in Section 4.1.

The limitation in the temporal coverage of the two products currently hinders the long time series of applications of NTL data. Although NTL observations from VIIRS/DNB provide a greater potential in monitoring human activities and environmental changes, the temporal coverage of available observations is shorter compared to the version 4 DMSP stable NTL composites. VIIRS/DNB NTL imageries were not released until 2012, while the DMSP-OLS ceased operation in 2013. Therefore, the version 4 DMSP time series NTL composite is the currently most widely used dataset of NTL for the analyses of time series [16,224]. However, this advantage of DMSP data will gradually decrease as the continuously-updated monthly VIIRS/DNB composite starts to play a more significant role in time series analyses.

Current NTL remote sensing applications still lack a long-term and consistent NTL dataset globally, back to 1990s. Such integrated datasets spanning 1992 to present will make it possible for long-term monitoring of human activities with low costs from the regional to global scales. A few studies have started to conduct analyses of time series using both DMSP and VIIRS. For example, a linear regression model was used to calibrate the raw daily DMSP images over Dome C in the Antarctic into VIIRS-like data by deriving the characteristic of DMSP DN and VIIRS radiance of the region of interest [225]. An inter-calibration model [118], designed for non-saturated urban areas, was proposed to calibrate the monthly VIIRS data into monthly DMSP-like data for estimating the city light dynamics during the war. Additionally, a power function model [98] was used to simulate the DMSP-like TNL from VIIRS TNL based on their quantitative relationship for investigating the dynamic of provincial GDP in China. Recently, with radiance-calibrated DMSP data and VIIRS data, a cross-sensor calibration model was proposed to generate DMSP-like VIIRS data. These attempts have contributed to enhancing the consistency of NTL or NTL indices between DMSP and VIIRS data; however, limitations still exist regarding the wide application of current methods. First, the datasets used are inaccessible to the general public [118,225], making these methods difficult for widespread applications in other regions. Second, the consistent NTL generated still has a limited temporal coverage [226], and the potential of the historical NTL archive has not been fully explored. Third, the models proposed could be robust

for specific lit areas [118], meaning that cautions are warranted when applying them in other regions. Considering that current methods cannot be widely applied and promoted, it is still a challenge to generate a long time series of consistent and comparable nighttime light dataset from 1992 to present.

4.3. Limited Understanding of Nighttime Lights for Perceiving the Changing World

Limited understanding of NTLs for perceiving the changing world hinders the in-depth analyses of NTLs on capturing accurate nightscape dynamics, characterizing real human activities and environment changes, and revealing or explaining potential social, economic, religious, and political issues. These limitations, mainly due to the deficiencies from current methods or data products, can be grouped into four aspects.

First, the pixel-level relationship between NTLs and land features/human activities has not been fully explored. Although the NTL magnitude and spatial patterns show potentials in characterizing the patterns and dynamics of human activities from local to global scales, the lack of distinct texture information makes it a challenge for accurately investigating various human activities using NTL over space at a finer scale. Currently, the multi-source remote sensing data, such as AVHRR, MODIS, SPOT VEGETATION, Landsat, and Sentinel-2, with detailed information of the landscape and ground features, have been used in NTL studies for two purposes: (1) Validating the extracted results from NTL data, such as urban extents [82,88,227,228]; and (2) improving the quality of NTL data or derivative results [43,214,229,230]. These attempts, either focusing on studies using coarse resolution NTL data, or using fine resolution data but still emphasizing the regional dynamics, cannot well explain how NTL signals respond to various land-use/land-cover types and socioeconomic activities such as population distribution, energy consumption, and building density. A clear understanding of the relationship between lit pixels and corresponding features of land surface and human activities is crucially important for further applications of nighttime light data. However, such a fundamental issue has not been fully addressed in previous studies.

Second, methods and algorithms for quantitatively characterizing human activities still need improvements. On the one hand, the under- and over-estimation of the intensity of human activities, such as urban extent [72,75], socioeconomic variables [111,114], fishing extent, energy use [153,231], and emissions [147,158], indicates that more efforts are needed to improve the accuracy and reliability of the results. On the other hand, the variations of thresholds, relationships, trends, and patterns of the extracted information from NTL imagery across different years/scales/extents [19] also suggest the necessity of automatic and intelligent methods in these studies. Although some robust relationships among the NTL signals, such as the quadratic relationship between the pixel-level NTL radiance and corresponding brightness gradient [232], and the quantile-based relationship between urban and rural NTLs [75], have been identified as effective ways for the large-scale urban mapping, these methods are only proven to be suitable for DMSP imagery. More efforts are needed to evaluate the applicability of these methods for other NTL data and to develop more effective methods.

Additionally, compared to monitoring of human activities, studies on revealing environmental changes are relatively limited. NTL data provide a cost-effective way for detecting the Earth's lights at night and tracking their changes over time. The quantitative monitoring of Earth at night cannot only be used to characterize human activities such as urbanization and conflicts, but also to provide a new perspective for understanding environmental changes. However, the latter is still limited, mainly because of the scale mismatch between current NTL data and the studied issues. The studies on environmental changes, which are geographic-specific issues, are mostly performed at the fine scale. Compared to human activity monitoring at the large scale, the early launched sensors (e.g., DMSP and VIIRS), which provide large scale lightscape with only single spectral band information, have limited capability of lighting detection, and therefore, cannot provide enough information required in environmental change studies. NTL data with higher spatial, temporal, and radiometric resolutions and multi-spectral band information are highly needed, particularly in future studies of environmental change.

Finally, the inconsistency between the derived information from NTL data and the actual status of human activities exists. The first type of difference comes from the sensor or data products. Although there are high correlations between anthropogenic NTL emissions and human activities, NTL is only one of the indicators for human activities. For example, no lighting does not mean there is no human activity. Moreover, different overpass times of NTL sensors have a certain impact on the detection of lighting on the Earth due to the varying dynamic of night lights, especially before and after the peaking lighting [27]. Especially, because of the various degrees of difference in overall sky brightness at night caused by this intra-night dynamic of different light sources (e.g., streetlights, lit windows of homes and shops, and vehicles) [53,220], it is likely to obtain a different nightscape from NTL images collected at different times. In addition, due to a combination of light scattering, instrumental effects, processing effects, and skyglow [233–235], the blooming effect is especially severe in DMSP-OLS data [221], and is more pervasive over areas nearby water and snow [19]. Besides, the lighting spectrum also affects the ability of existing sensors to quantify artificial lights from space. This limitation even exists in VIIRS data, which lack the capability to capture blue light from white-light emitting diodes (LEDs) [236]. Last, the different imaging angles could also affect the visibility of facade lighting and detection sensitivity of satellite sensors to different sources of radiation (e.g., illuminated signs and parking lot lighting) [237], especially when the spatial resolution of sensors is high. Some directional light sources, such as searchlights and car headlights, cannot be detected [53]. This effect could limit the ability of NTL sensors to capture the lighting changes. Therefore, due to these uncertainties caused by sensors and products, understanding how to maximize the usefulness of existing and future NTL observations to capture the real lighting change and characterize specific human activities is still a challenge. The second type of difference comes from the methods of investigating human activities. As responses of changes in NTL to human activities vary over space and time, analyses without considering sociocultural, lighting sources, outliers, and a sizeable portion of dark or dim areas could lead to biases of estimated human activities [19]. The variations of NTL response make the comparison across space and time challenging, and present a barrier to quantifying and understanding the dynamic of human activities. Causes of observed light changes across space and time, which are crucial for investigating the relationship between NTL observations and human activities, however, are still limitedly considered in previous studies.

5. Strategic Directions for Nighttime Light Remote Sensing Research

According to challenges and limitations of current NTL remote sensing applications, four key advancements are recommended (Figure 4). First, NTL observations with higher spatial resolution, wider radiometric detection range, and multi-spectral bands are needed from improvements in both the widely used, newly updated, and future released satellites/sensors/products. Second, it is of great significance to develop a long time series of consistent NTL dataset by integrating current NTL composites for monitoring spatiotemporal dynamics of human activities over a sufficiently long period of time and for evaluating related environmental changes. Third, it will provide great potentials for detecting changes and understanding driving causes by integrating NTL data with other data, including not only commonly used remote sensing data, but also geo-located big data, field data, social media data, expert knowledge, and local experience. Finally, more attention should be paid to multidisciplinary and interdisciplinary analyses of NTLs, including not only analyses on human activities, but also studies on environment changes.
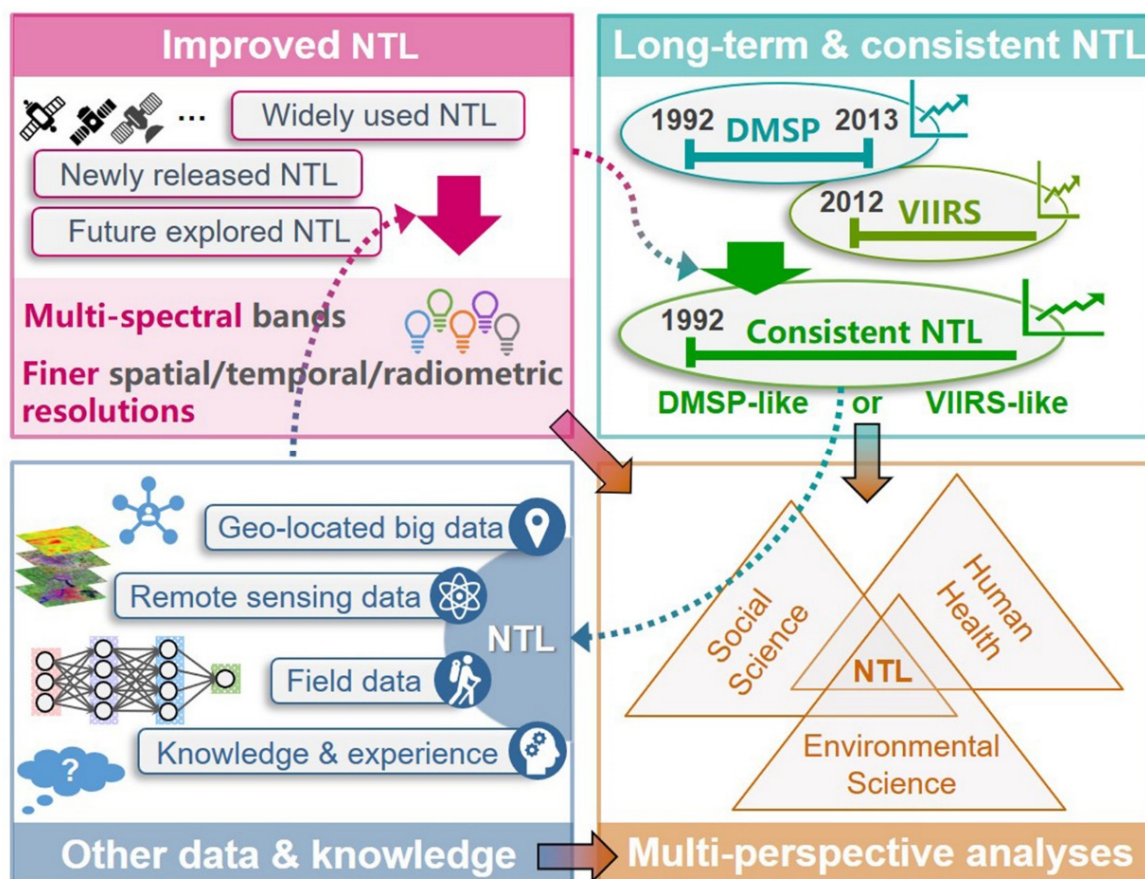
Figure 4. Strategic directions for future NTL remote sensing research.

5.1. Improving Nighttime Light Data

Future applications of NTL remote sensing require improved sensors and data products for mining accurate and rich information from future NTL observations. With these improvements, it is expected that NTL observations with significant improvements in spatial, temporal, radiometric, and spectral resolutions will be available. The improved NTL observations, with strong capabilities for capturing nightscape dynamics, will open new avenues for monitoring human activities and environment changes at the fine spatiotemporal scales.

First, more efforts are needed to mitigate the saturation and blooming effects that exist in the version 4 DMSP stable NTL composites. In addition to land surface features and demographic information, socio-media data, such as volunteered data or mobile-based check-in data, is expected—as a new data source—to reveal more details in saturated NTL pixels. New methods of deburring DMSP-OLS data, independent of auxiliary data such as NDVI or land classification, are expected to mitigate the blooming effect of DMSP-OLS data. Meanwhile, further comparisons between DMSP-OLS and VIIRS/DNB data from different perspectives, such as the response of NTL to land surface features or population density, could also promote a deeper understanding of differences of the derived information from the two products. These differences are key for improving NTL observations. With the improvement in NTL data and the derived information, capturing better capture human activities and environment changes is more promising.

Second, NTL observations with higher spatial, temporal, and radiometric resolutions are needed. Currently, most studies of NTLs have not been able to characterize spatial patterns at the neighborhood and street level due to the lack of freely-available observations with fine spatial and radiometric resolution. Considering that the price of fine (e.g., submeter level) NTL images offered by commercial satellites (e.g., Israeli EROS-B and Chinese JL1) is high, the recent launch of the Luojia-1 cuebsat

with free data access for monitoring the fine-scale artificial light at night could promote more novel applications. Compared to the monthly and seasonal changes in anthropogenic light-emitting activities, for light-emitting activities with a short duration but potentially high social or environmental impact, the timely monitoring of high frequent human activities such as wars and disasters [48] also put new demands on the improvement of the temporal resolutions of NTL data. For instance, the recently released Black Marble product provides another step forward in monitoring light-emitting activities at daily intervals, which is of great significance for assessing the intensity and loss of disasters and conflicts. With the consistent emergence and improvement of sensors and products, NTL composites with higher spatial, temporal, and radiometric resolutions are expected to be used to monitor the spatiotemporal dynamics of the nightscape.

Third, identifying different types of lighting will greatly benefit from the multi-spectral information of future NTL data. As the emission spectra of artificial lighting sources are different [238], the major types of artificial lighting sources can be separated by the use of hyperspectral data [239–241]. Such information will be of help for evaluating the impact of light pollution and mapping the spatial structure of human activities. However, the majority of current satellite NTL sensors are panchromatic, except for ISS photos and JL-1 satellite which offer RGB color images. As mentioned, the lack of sensitivity to blue light from LEDs affects the ability of existing sensors, such as VIIRS/DNB, to quantify artificial lights from space, which will lead to a serious missing of important spectral information when more cities change their street lighting technology to LEDs, especially in the United Kingdom [53]. Blue and other spectral bands in the range from visible to near-infrared are needed in future NTL sensors. New and improved sensors and algorithms with multi- or hyperspectral bands will play a more important role in visualizing, identifying, and quantifying changes in light emissions and pollution.

5.2. Developing a Long Time Series of Consistent Nighttime Light Data

A continuous and consistent monitoring of global nightscape from space will provide precious records of human activities from past to future. With the spatially-explicit observations of artificial lighting sources across human settlements at night, the intensity of human activities can be quantified, providing the basic knowledge needed for understanding the environment changes and impacts of light emissions related to human activities worldwide [184]. The quantification and characterization of human activities and environment changes using NTL data provide us a cost-effective way for perceiving the changing world from different aspects. These aspects include—but are not limited to—urbanization, socioeconomic activities, conflicts and disasters, fisheries, energy use and greenhouse gas emissions, human health, and the ecosystem. Therefore, a long-term record of the global nightscape is of great significance for perceiving our changing world.

Long-term and consistent NTL data, from past to present, even the future, is a pressing need for the continuous and consistent monitoring of human activities from regional to global scales. The version 4 annual stable NTL dataset from DMSP and the version 1 suite of monthly and annual NTL composites from VIIRS will play a key role in the generation of the new time series product. Although a few studies have contributed to enhancing the consistency of NTL signals from different datasets, the integration of DMSP and VIIRS datasets at the pixel level is still challenging and the related product is still lacking. Therefore, more efforts are needed in developing a long time series of consistent NTL data from the 1990s onwards.

Addressing the inconsistency problem between DMSP-OLS and NPP-VIIRS is the key for developing a long time series of consistent NTL data. This inconsistency of NTL data between DMSP-OLS and NPP-VIIRS could be partly reduced by calibrating VIIRS into DMSP-like data, or improving DMSP into VIIRS-like data. Future efforts to mitigate the saturation and blooming effects of DMSP stable NTL data will greatly promote the comparability of the two datasets. Similarly, the comparability of the two datasets can also be achieved by aggregating VIIRS into DMSP-like data. With these efforts, the spatial pattern of the processed NTL from DMSP and VIIRS will become more consistent. In addition to reducing the inconsistency caused by sensor performance for spatial and radiometric resolutions,

the NTL differences of DMSP and VIIRS caused by their different overpass time should be paid more attention when developing a long time series of consistent DMSP-like or VIIRS-like NTL data.

5.3. Integrating Nighttime Light Observations with Other Data and Knowledge

Integrating NTL observations with geo-located big data, multi-spectral/sourced remote sensing data, and field data will provide more opportunities for NTL remote sensing studies. The added information from these data will contribute to perceiving human activities and related environment changes from different perspectives. In addition to validating extracted information from NTL observations, the responses of light signals to ground features and different human activities, such as population dynamics derived from socio-media data, can be better understood by integrating other relevant data. Moreover, field data, acquired through site-specific analyses, is another way to investigate the unusual dynamics of lightscape and help reveal their drivers. Therefore, more attention in the use of these multi-source datasets and knowledge is needed for monitoring NTL dynamics, identifying human activities, and exploring their potential causes.

The integration of NTL observations with daytime satellite imageries can serve as useful training inputs of deep learning algorithms for characterizing and predicting human activities. Daytime satellite imageries, with abundant information about landscape features, provide great potentials for characterizing the structure of human activities. NTL data record the light brightness of the Earth at night, and are considered as a rough proxy of the intensity of human activities. A combination of these two types of observations to label and train deep learning models is of great potential to capture both the structure and intensity information of human activities. For example, with a novel machine learning approach [108,242], the combined information from NTL and high-resolution daytime images have been demonstrated to be helpful for estimating socioeconomic activities (e.g., household consumption and assets), and make it possible for tracking poverty status in developing countries. The transfer learning strategy used here provides a new insight for NTL studies. More efforts are needed to broaden NTL applications in deep learning by integrating NTL data and daytime images, especially when more fine NTL images become available.

Integrating expert knowledge and local experiences into analyses on NTL data is promising for understanding the detected dynamics of lightscape at night and revealing the causes of their changes. The nighttime lightscape, related to economic activities, urbanization, and lighting types, always varies between countries, regions, and cities over time. These variations of NTL across space and time could present a barrier to the understanding of responses of light signals to human activities. For instance, NTL images may not be able to capture urban dynamics in some regions with weak luminosity at night due to the limited capacity of power supplies [34] or the policy of streetlights [53]. Expert knowledge and local experiences may help reveal the underlying mechanisms of the variations and provide more insights into the dynamics of human activities. For example, factors such as the history of development were used to explain the rapid increases of NTL intensities in some geographic clusters in China [243]. Therefore, caution is needed when analyzing geographic and socioeconomic phenomena using NTL data, and the integration of social, economic, cultural, political, historical, and even religious background of study areas, as well as special expertise in related fields with NTL remote sensing, could be of great help.

5.4. Promoting Multidisciplinary and Interdisciplinary Analyses of Nighttime Lights

Promoting multidisciplinary and interdisciplinary analyses of NTLs is of great significance for exploring the potential of NTL remote sensing. First, it broadens applications of NTL from human dimensions to environmental change. Second, it improves the understanding of NTL changes by revealing potential socioeconomic or environmental issues and tracking possible causes. Multidisciplinary and interdisciplinary analyses of NTL are needed from different disciplines, such as environmental science, social science, and human health, to further explore the potential of NTL.

First, more efforts are needed to reveal the impacts of NTL on environment and species ecology. In previous studies, quantitative indicators such as TNL, NTM, and NTSD have been used to reflect trends of light pollution. However, these indicators cannot capture the details of complex environmental issues such as climate changes or ecological processes. Therefore, analysis of NTL research from a broader range of disciplines, including biology and ecology, could benefit researchers with a thorough understanding of ecological impacts of NTL. For example, multidisciplinary and interdisciplinary analyses can help identify intensity thresholds, which have significant ecological implications, and investigate impacts of light at population and ecosystem levels such as mortality and fecundity rates, species composition, and trophic structure.

Second, disciplinary knowledge of social science, such as regional politics, economics, and religion, are needed for analyzing the phenomena revealed by the lightscape dynamic. NTL only provides the measurement of night light emissions, while further exploration of the relationships between NTL and social science indicators could better demonstrate how social and economic variables interact and respond to lights. The most significant progress from previous studies is that GDP and its growth rate have been estimated using socioeconomic and NTL data and econometric models. It is highly needed, in future research, to integrate more social science indicators into NTL for understanding the factors of observed lights and their changes, which could be of great importance for light pollution mitigation.

Third, more attention and investigation are needed for human health effects of NTL. Most previous studies have investigated the interactions between indoor artificial light exposure at night and human health, by measuring indoor lighting habits at individual exposure levels. Results showed that indoor artificial light increased the risks in cancer and circadian disruption, while studies regarding health effects of the outdoor illumination levels are still limited. Some experimental studies have reported that brighter outdoor lighting induces greater health effects. However, further studies are still highly needed. For example, the thresholds of outdoor light intensity and exposure time that cause human health effects remain unknown. Therefore, further studies, such as the association between NTL and health consequences, are of crucial significance to develop strategies to protect human beings from artificial light-induced diseases.

6. Conclusions

This review aimed at summarizing applications of NTL satellite remote sensing and how NTL data, at the current stage and in future, contribute to perceiving, characterizing, and quantifying changes of the Earth. Owing to continuously updated and improved sensors and data products of NTL, various applications of satellite-based NTL remote sensing have been emerging since the late 1990s. These studies greatly promote and deepen our understanding of urbanization and socioeconomic dynamics, armed conflicts and disasters, fishery activities, greenhouse gas emissions and energy use consumption, and light pollution and health effects. However, due to the limitations of the capability of sensors for detecting low lighting at night, and the unsolved issues of algorithms and technologies in data generation and processing, challenges and difficulties still exist in the access to long-term consistent NTL data with a high quality. These challenges hinder the further applications of NTL remote sensing for perceiving the changing world. Future research on satellite remote sensing of NTL requires improved sensors and data products for acquiring accurate and rich information, especially when the era of white LEDs is coming. A consistent and continuous NTL dataset is also of pressing need for long-term monitoring of human activities from regional to global scales, which is of significance for revealing potential socioeconomic, human, and environmental issues. In addition to the improvement of data products, the combination of NTL observations with other data, either remote sensing data, social media data, field data, or expert knowledge and local experiences, is promising for comprehensively characterizing and understanding the changes of human activities. Finally, the in-depth analyses from a multidisciplinary or interdisciplinary perspective are of great importance for revealing the possible causes and potential impacts behind the lighting changes.

Conflicts of Interest: The authors declare no conflicts of interest.

References

1. Council, N.R. *Understanding the Changing Planet: Strategic Directions for the Geographical Sciences*; National Academies Press: Washington, DC, USA, 2010.
2. Defries, R.S.; Bounoua, L.; Collatz, G.J. Human modification of the landscape and surface climate in the next fifty years. *Glob. Chang. Biol.* **2002**, *8*, 438–458. [CrossRef]
3. Wannebo, A.V.; Sanderson, E.W.; Woolmer, G.; Redford, K.H.; Jaiteh, M.; Levy, M.A. The Human Footprint and the Last of the Wild: The human footprint is a global map of human influence on the land surface, which suggests that human beings are stewards of nature, whether we like it or not. *BioScience* **2002**, *52*, 891–904.
4. Chuvieco, E. *Earth Observation of Global Change: The Role of Satellite Remote Sensing in Monitoring the Global Environment*; Springer: Berlin/Heidelberg, Germany, 2008.
5. Elvidge, C.D.; Baugh, K.E.; Anderson, S.J.; Sutton, P.C.; Ghosh, T. The Night Light Development Index (NLDI): A spatially explicit measure of human development from satellite data. *Soc. Geogr.* **2012**, *7*, 23–35. [CrossRef]
6. Chen, X.; Nordhaus, W.D. Using luminosity data as a proxy for economic statistics. *Proc. Natl. Acad. Sci. USA* **2011**, *108*, 8589–8594. [CrossRef] [PubMed]
7. Doll, C.N.H.; Muller, J.-P.; Morley, J.G. Mapping regional economic activity from night-time light satellite imagery. *Ecol. Econ.* **2006**, *57*, 75–92. [CrossRef]
8. He, C.; Shi, P.; Li, J.; Chen, J.; Pan, Y.; Li, J.; Zhuo, L.; Ichinose, T. Restoring urbanization process in China in the 1990s by using non-radiance-calibrated DMSP/OLS nighttime light imagery and statistical data. *Chin. Sci. Bull.* **2006**, *51*, 1614–1620. [CrossRef]
9. Roman, M.O.; Stokes, E.C. Holidays in lights: Tracking cultural patterns in demand for energy services. *Earths Future* **2015**, *3*, 182–205. [CrossRef]
10. Yu, B.; Shi, K.; Hu, Y.; Huang, C.; Chen, Z.; Wu, J. Poverty Evaluation Using NPP-VIIRS Nighttime Light Composite Data at the County Level in China. *IEEE J. Sel. Top. Appl. Earth Obs. Remote Sens.* **2015**, *8*, 1217–1229. [CrossRef]
11. Zheng, Q.; Deng, J.; Jiang, R.; Wang, K.; Xue, X.; Lin, Y.; Huang, Z.; Shen, Z.; Li, J.; Shahtahmassebi, A.R. Monitoring and assessing "ghost cities" in Northeast China from the view of nighttime light remote sensing data. *Habitat Int.* **2017**, *70*, 34–42. [CrossRef]
12. Kamrowski, R.L.; Limpus, C.; Jones, R.; Anderson, S.; Hamann, M. Temporal changes in artificial light exposure of marine turtle nesting areas. *Glob. Chang. Biol.* **2014**, *20*, 2437–2449. [CrossRef]
13. Jiang, W.; He, G.; Leng, W.; Long, T.; Wang, G.; Liu, H.; Peng, Y.; Yin, R.; Guo, H. Characterizing Light Pollution Trends across Protected Areas in China Using Nighttime Light Remote Sensing Data. *ISPRS Int. Geo-Inf.* **2018**, *7*, 243. [CrossRef]
14. Zhao, M.; Cheng, W.; Zhou, C.; Li, M.; Huang, K.; Wang, N. Assessing Spatiotemporal Characteristics of Urbanization Dynamics in Southeast Asia Using Time Series of DMSP/OLS Nighttime Light Data. *Remote Sens.* **2018**, *10*, 47. [CrossRef]
15. Li, X.; Zhou, Y. Urban mapping using DMSP/OLS stable night-time light: A review. *Int. J. Remote Sens.* **2017**, *38*, 6030–6046. [CrossRef]
16. Huang, Q.; Yang, X.; Gao, B.; Yang, Y.; Zhao, Y. Application of DMSP/OLS Nighttime Light Images: A Meta-Analysis and a Systematic Literature Review. *Remote Sens.* **2014**, *6*, 6844–6866. [CrossRef]
17. Hu, K.; Qi, K.; Guan, Q.; Wu, C.; Yu, J.; Qing, Y.; Zheng, J.; Wu, H.; Li, X. A scientometric visualization analysis for night-time light remote sensing research from 1991 to 2016. *Remote Sens.* **2017**, *9*, 802. [CrossRef]
18. Doll, C.N. *CIESIN Thematic Guide to Night-Time Light Remote Sensing and Its Applications*; Center for International Earth Science Information Network (CIESIN): Palisades, NY, USA, 2008.

19. Bennett, M.M.; Smith, L.C. Advances in using multitemporal night-time lights satellite imagery to detect, estimate, and monitor socioeconomic dynamics. *Remote Sens. Environ.* **2017**, *192*, 176–197. [CrossRef]

20. Cho, Y.; Ryu, S.H.; Lee, B.R.; Kim, K.H.; Lee, E.; Choi, J. Effects of artificial light at night on human health: A literature review of observational and experimental studies applied to exposure assessment. *Chronobiol. Int.* **2015**, *32*, 1294–1310. [CrossRef]

21. Zhang, Q.; Levin, N.; Chalkias, C.; Letu, H. *Nighttime Light Remote Sensing—Monitoring Human Societies from Outer Space*; Thenkabail, P.S., Ed.; Taylor & Francis Inc.: Abingdon-on-Thames, UK, 2015; p. 289e310.

22. Li, D.; Zhao, X.; Li, X. Remote sensing of human beings—A perspective from nighttime light. *Geo-Spat. Inf. Sci.* **2016**, *19*, 69–79. [CrossRef]

23. Elvidge, C.D.; Baugh, K.E.; Dietz, J.B.; Bland, T.; Sutton, P.C.; Kroehl, H.W. Radiance calibration of DMSP-OLS low-light imaging data of human settlements. *Remote Sens. Environ.* **1999**, *68*, 77–88. [CrossRef]

24. Li, X.; Zhou, Y. A stepwise calibration of global DMSP/OLS stable nighttime light data (1992–2013). *Remote Sens.* **2017**, *9*, 637.

25. Baugh, K.; Elvidge, C.D.; Ghosh, T.; Ziskin, D. Development of a 2009 Stable Lights Product using DMSP-OLS data. *Proc. Asia-Pac. Adv. Netw.* **2010**, *30*, 114. [CrossRef]

26. Elvidge, C.D.; Imhoff, M.L.; Baugh, K.E.; Hobson, V.R.; Nelson, I.; Safran, J.; Dietz, J.B.; Tuttle, B.T. Night-time lights of the world: 1994–1995. *ISPRS-J. Photogramm. Remote Sens.* **2001**, *56*, 81–99. [CrossRef]

27. Elvidge, C.D.; Baugh, K.E.; Zhizhin, M.; Hsu, F.-C. Why VIIRS data are superior to DMSP for mapping nighttime lights. *Proc. Asia-Pac. Adv. Netw.* **2013**, *35*, 62. [CrossRef]

28. Elvidge, C.D.; Baugh, K.E.; Kihn, E.A.; Kroehl, H.W.; Davis, E.R. Mapping city lights with nighttime data from the DMSP Operational Linescan System. *Photogramm. Eng. Remote Sens.* **1997**, *63*, 727–734.

29. Ziskin, D.; Baugh, K.; Hsu, F.-C.; Elvidge, C.D. Methods Used For the 2006 Radiance Lights. *Proc. Asia-Pac. Adv. Netw.* **2010**, *30*, 131. [CrossRef]

30. Hsu, F.-C.; Baugh, K.; Ghosh, T.; Zhizhin, M.; Elvidge, C. DMSP-OLS Radiance Calibrated Nighttime Lights Time Series with Intercalibration. *Remote Sens.* **2015**, *7*, 1855–1876. [CrossRef]

31. Waluda, C.; Yamashiro, C.; Elvidge, C.; Hobson, V.; Rodhouse, P. Quantifying light-fishing for Dosidicus gigas in the eastern Pacific using satellite remote sensing. *Remote Sens. Environ.* **2004**, *91*, 129–133. [CrossRef]

32. Badarinath, K.; Sharma, A.; Kharol, S. Forest fire monitoring and burnt area mapping using satellite data: a study over the forest region of Kerala State, India. *Int. J. Remote Sens.* **2011**, *32*, 85–102. [CrossRef]

33. Filho, C.D.S.; Zullo, J., Jr.; Elvidge, C. Brazil's 2001 energy crisis monitored from space. *Int. J. Remote Sens.* **2004**, *25*, 2475–2482. [CrossRef]

34. Min, B.; Gaba, K. Tracking Electrification in Vietnam Using Nighttime Lights. *Remote Sens.* **2014**, *6*, 9511–9529. [CrossRef]

35. Hillger, D.; Kopp, T.; Lee, T.; Lindsey, D.; Seaman, C.; Miller, S.; Solbrig, J.; Kidder, S.; Bachmeier, S.; Jasmin, T.; et al. First-Light Imagery from Suomi NPP VIIRS. *Bull. Am. Meteorol. Soc.* **2013**, *94*, 1019–1029. [CrossRef]

36. Liao, L.B.; Weiss, S.; Mills, S.; Hauss, B. Suomi NPP VIIRS day-night band on-orbit performance. *J. Geophys. Res. Atmos.* **2013**, *118*, 12705–12718. [CrossRef]

37. Miller, S.; Straka, W.; Mills, S.; Elvidge, C.; Lee, T.; Solbrig, J.; Walther, A.; Heidinger, A.; Weiss, S. Illuminating the Capabilities of the Suomi National Polar-Orbiting Partnership (NPP) Visible Infrared Imaging Radiometer Suite (VIIRS) Day/Night Band. *Remote Sens.* **2013**, *5*, 6717–6766. [CrossRef]

38. Liang, C.K.; Mills, S.; Hauss, B.I.; Miller, S.D. Improved VIIRS day/night band imagery with near-constant contrast. *IEEE Trans. Geosci. Remote Sens.* **2014**, *52*, 6964–6971. [CrossRef]

39. Miller, S.D.; Mills, S.P.; Elvidge, C.D.; Lindsey, D.T.; Lee, T.F.; Hawkins, J.D. Suomi satellite brings to light a unique frontier of nighttime environmental sensing capabilities. *Proc. Natl. Acad. Sci. USA* **2012**, *109*, 15706–15711. [CrossRef] [PubMed]

40. Baugh, K.; Hsu, F.-C.; Elvidge, C.D.; Zhizhin, M. Nighttime Lights Compositing Using the VIIRS Day-Night Band: Preliminary Results. *Proc. Asia-Pac. Adv. Netw.* **2013**, *35*, 70. [CrossRef]

41. Mills, S.; Weiss, S.; Liang, C. VIIRS day/night band (DNB) stray light characterization and correction. In Proceedings of the Earth Observing Systems XVIII, San Diego, CA, USA, 25–29 August 2013.

42. Elvidge, C.D.; Baugh, K.; Zhizhin, M.; Hsu, F.C.; Ghosh, T. VIIRS night-time lights. *Int. J. Remote Sens.* **2017**, *38*, 5860–5879. [CrossRef]

43. Ma, T.; Zhou, C.; Pei, T.; Haynie, S.; Fan, J. Responses of Suomi-NPP VIIRS-derived nighttime lights to socioeconomic activity in China's cities. *Remote Sens. Lett.* **2014**, *5*, 165–174. [CrossRef]

44. Zhao, M.; Cheng, W.; Zhou, C.; Li, M.; Wang, N.; Liu, Q. GDP Spatialization and Economic Differences in South China Based on NPP-VIIRS Nighttime Light Imagery. *Remote Sens.* **2017**, *9*, 673. [CrossRef]

45. Li, X.; Xu, H.; Chen, X.; Li, C. Potential of NPP-VIIRS Nighttime Light Imagery for Modeling the Regional Economy of China. *Remote Sens.* **2013**, *5*, 3057–3081. [CrossRef]

46. Shi, K.; Yu, B.; Hu, Y.; Huang, C.; Chen, Y.; Huang, Y.; Chen, Z.; Wu, J. Modeling and mapping total freight traffic in China using NPP-VIIRS nighttime light composite data. *GISci. Remote Sens.* **2015**, *52*, 274–289. [CrossRef]

47. Román, M.O.; Wang, Z.; Shrestha, R.; Yao, T.; Kalb, V. *Black Marble User Guide Version 1.0*; NASA: Washington, DC, USA, 2019.

48. Román, M.O.; Wang, Z.; Sun, Q.; Kalb, V.; Miller, S.D.; Molthan, A.; Schultz, L.; Bell, J.; Stokes, E.C.; Pandey, B.; et al. NASA's Black Marble nighttime lights product suite. *Remote Sens. Environ.* **2018**, *210*, 113–143. [CrossRef]

49. Wang, Z.; Shrestha, R.; Román, M. NASA's Black Marble Nighttime Lights Product Suite Algorithm Theoretical Basis Document (ATBD). Version 1.0; 2018. Available online: https://viirsland.gsfc.nasa.gov/PDF/VIIRS_BlackMarble_ATBD_V1.0.pdf (accessed on 10 August 2019).

50. Wang, Z.; Román, M.O.; Sun, Q.; Molthan, A.L.; Schultz, L.A.; Kalb, V.L. Monitoring Disaster-Related Power Outages Using Nasa Black Marble Nighttime Light Product. *ISPRS Int. Arch. Photogramm. Remote Sens. Spat. Inf. Sci.* **2018**, *XLII-3*, 1853–1856. [CrossRef]

51. Román, M.O.; Stokes, E.C.; Shrestha, R.; Wang, Z.; Schultz, L.; Carlo, E.A.S.; Sun, Q.; Bell, J.; Molthan, A.; Kalb, V. Satellite-based assessment of electricity restoration efforts in Puerto Rico after Hurricane Maria. *PLoS ONE* **2019**, *14*, e0218883. [CrossRef] [PubMed]

52. De Miguel, A.S.; Castaño, J.G.; Zamorano, J.; Pascual, S.; Ángeles, M.; Cayuela, L.; Martinez, G.M.; Challupner, P.; Kyba, C.C. Atlas of astronaut photos of Earth at night. *Astron. Geophys.* **2014**, *55*, 4.36. [CrossRef]

53. Kyba, C.; Garz, S.; Kuechly, H.; de Miguel, A.; Zamorano, J.; Fischer, J.; Hölker, F. High-Resolution Imagery of Earth at Night: New Sources, Opportunities and Challenges. *Remote Sens.* **2015**, *7*, 1–23. [CrossRef]

54. Kotarba, A.Z.; Aleksandrowicz, S. Impervious surface detection with nighttime photography from the International Space Station. *Remote Sens. Environ.* **2016**, *176*, 295–307. [CrossRef]

55. Wicht, M.; Kuffer, M. The continuous built-up area extracted from ISS night-time lights to compare the amount of urban green areas across European cities. *Eur. J. Remote Sens.* **2019**, *52*, 58–73. [CrossRef]

56. Kuffer, M.; Sliuzas, R.; van Maarseveen, M.; Pfeffer, K.; Baud, I. City nighttime light variations using ISS images. In Proceedings of the 2017 Joint Urban Remote Sensing Event (JURSE), Dubai, UAE, 6–8 March 2017; pp. 1–4.

57. Metcalf, J.P. *Detecting and Characterizing Nighttime Lighting Using Multispectral and Hyperspectral Imaging*; Naval Postgraduate School: Monterey, CA, USA, 2012.

58. Mazor, T.; Levin, N.; Possingham, H.P.; Levy, Y.; Rocchini, D.; Richardson, A.J.; Kark, S. Can satellite-based night lights be used for conservation? The case of nesting sea turtles in the Mediterranean. *Biol. Conserv.* **2013**, *159*, 63–72. [CrossRef]

59. Pauwels, J.; Le Viol, I.; Azam, C.; Valet, N.; Julien, J.F.; Bas, Y.; Lemarchand, C.; Sanchez de Miguel, A.; Kerbiriou, C. Accounting for artificial light impact on bat activity for a biodiversity-friendly urban planning. *Landsc. Urban Plan.* **2019**, *183*, 12–25. [CrossRef]

60. Levin, N.; Duke, Y. High spatial resolution night-time light images for demographic and socio-economic studies. *Remote Sens. Environ.* **2012**, *119*, 1–10. [CrossRef]

61. Li, K.; Chen, Y.; Li, Y. The Random Forest-Based Method of Fine-Resolution Population Spatialization by Using the International Space Station Nighttime Photography and Social Sensing Data. *Remote Sens.* **2018**, *10*, 1650. [CrossRef]

62. Kuffer, M.; Pfeffer, K.; Sliuzas, R.; Taubenböck, H.; Baud, I.; van Maarseveen, M. Capturing the urban divide in nighttime light images from the International Space Station. *IEEE J. Sel. Top. Appl. Earth Obs. Remote Sens.* **2018**, *11*, 2578–2586. [CrossRef]

63. Levin, N.; Johansen, K.; Hacker, J.M.; Phinn, S. A new source for high spatial resolution night time images—The EROS-B commercial satellite. *Remote Sens. Environ.* **2014**, *149*, 1–12. [CrossRef]

64. Zheng, Q.; Weng, Q.; Huang, L.; Wang, K.; Deng, J.; Jiang, R.; Ye, Z.; Gan, M. A new source of multi-spectral high spatial resolution night-time light imagery—JL1-3B. *Remote Sens. Environ.* **2018**, *215*, 300–312. [CrossRef]

65. Van Doren, B.M.; Horton, K.G.; Dokter, A.M.; Klinck, H.; Elbin, S.B.; Farnsworth, A. High-intensity urban light installation dramatically alters nocturnal bird migration. *Proc. Natl. Acad. Sci. USA* **2017**, *114*, 11175–11180. [CrossRef] [PubMed]

66. Walczak, K.; Gyuk, G.; Kruger, A.; Byers, E.; Huerta, S. Nitesat: A high resolution, full-color, light pollution imaging satellite mission. *Int. J. Sustain. Lighting* **2017**, *19*, 48–55. [CrossRef]

67. Li, X.; Li, X.; Li, D.; He, X.; Jendryke, M. A preliminary investigation of Luojia-1 night-time light imagery. *Remote Sens. Lett.* **2019**, *10*, 526–535. [CrossRef]

68. Jiang, W.; He, G.; Long, T.; Guo, H.; Yin, R.; Leng, W.; Liu, H.; Wang, G. Potentiality of Using Luojia 1-01 Nighttime Light Imagery to Investigate Artificial Light Pollution. *Sensors* **2018**, *18*, 2900. [CrossRef]

69. Li, X.; Zhao, L.; Li, D.; Xu, H. Mapping Urban Extent Using Luojia 1-01 Nighttime Light Imagery. *Sensors* **2018**, *18*, 3665. [CrossRef]

70. Pack, D.W.; Hardy, B.S. CubeSat Nighttime Lights. In Proceedings of the 30th Annual AIAA/USU Conference on Small Satellites, Logan, UT, USA, 6–11 August 2016.

71. Zhou, Y.; Smith, S.J.; Elvidge, C.D.; Zhao, K.; Thomson, A.; Imhoff, M. A cluster-based method to map urban area from DMSP/OLS nightlights. *Remote Sens. Environ.* **2014**, *147*, 173–185. [CrossRef]

72. Zhou, Y.; Smith, S.J.; Zhao, K.; Imhoff, M.; Thomson, A.; Bond-Lamberty, B.; Asrar, G.R.; Zhang, X.; He, C.; Elvidge, C.D. A global map of urban extent from nightlights. *Environ. Res. Lett.* **2015**, *10*, 054011. [CrossRef]

73. Sharma, R.C.; Tateishi, R.; Hara, K.; Gharechelou, S.; Iizuka, K. Global mapping of urban built-up areas of year 2014 by combining MODIS multispectral data with VIIRS nighttime light data. *Int. J. Digit. Earth* **2016**, *9*, 1004–1020. [CrossRef]

74. He, C.; Liu, Z.; Gou, S.; Zhang, Q.; Zhang, J.; Xu, L. Detecting global urban expansion over the last three decades using a fully convolutional network. *Environ. Res. Lett.* **2019**, *14*, 034008. [CrossRef]

75. Zhou, Y.; Li, X.; Asrar, G.R.; Smith, S.J.; Imhoff, M. A global record of annual urban dynamics (1992–2013) from nighttime lights. *Remote Sens. Environ.* **2018**, *219*, 206–220. [CrossRef]

76. Chen, Z.; Yu, B.; Zhou, Y.; Liu, H.; Yang, C.; Shi, K.; Wu, J. Mapping Global Urban Areas From 2000 to 2012 Using Time-Series Nighttime Light Data and MODIS Products. *IEEE J. Sel. Top. Appl. Earth Obs. Remote Sens.* **2019**, *12*, 1143–1153. [CrossRef]

77. Liu, Z.; He, C.; Zhou, Y.; Wu, J. How much of the world's land has been urbanized, really? A hierarchical framework for avoiding confusion. *Landsc. Ecol.* **2014**, *29*, 763–771. [CrossRef]

78. Roy Chowdhury, P.; Maithani, S. Monitoring growth of built-up areas in indo-gangetic plain using multi-sensor remote sensing data. *J. Indian Soc. Remote Sens.* **2010**, *38*, 291–300. [CrossRef]

79. Shi, K.; Huang, C.; Yu, B.; Yin, B.; Huang, Y.; Wu, J. Evaluation of NPP-VIIRS night-time light composite data for extracting built-up urban areas. *Remote Sens. Lett.* **2014**, *5*, 358–366. [CrossRef]

80. Xie, Y.; Weng, Q. Updating urban extents with nighttime light imagery by using an object-based thresholding method. *Remote Sens. Environ.* **2016**, *187*, 1–13. [CrossRef]

81. Zhang, J.; Zhou, Z.; Shuai, G.; Liu, H. Support vector data description model to map urban extent from National Polar-Orbiting Partnership Satellite–Visible Infrared Imaging Radiometer Suite nightlights and normalized difference vegetation index. *J. Appl. Remote Sens.* **2016**, *10*, 026012. [CrossRef]

82. Henderson, M.; Yeh, E.T.; Gong, P.; Elvidge, C.; Baugh, K. Validation of urban boundaries derived from global night-time satellite imagery. *Int. J. Remote Sens.* **2003**, *24*, 595–609. [CrossRef]

83. Ju, C.; Zhou, X.; He, Q. On the application of a concentric zone model (CZM) for classifying and extracting urban boundaries using night-time stable light data in Urumqi of Xinjiang, China. *Remote Sens. Lett.* **2016**, *7*, 1033–1042. [CrossRef]

84. Sutton, P.C.; Anderson, S.J.; Elvidge, C.D.; Tuttle, B.T.; Ghosh, T. Paving the planet: Impervious surface as proxy measure of the human ecological footprint. *Prog. Phys. Geogr. Earth Environ.* **2009**, *33*, 510–527. [CrossRef]

85. Ma, Q.; He, C.; Wu, J.; Liu, Z.; Zhang, Q.; Sun, Z. Quantifying spatiotemporal patterns of urban impervious surfaces in China: An improved assessment using nighttime light data. *Landsc. Urban Plan.* **2014**, *130*, 36–49. [CrossRef]

86. Imhoff, M.L.; Lawrence, W.T.; Stutzer, D.C.; Elvidge, C.D. A technique for using composite DMSP/OLS "city lights" satellite data to map urban area. *Remote Sens. Environ.* **1997**, *61*, 361–370. [CrossRef]

87. Liu, Z.; He, C.; Zhang, Q.; Huang, Q.; Yang, Y. Extracting the dynamics of urban expansion in China using DMSP-OLS nighttime light data from 1992 to 2008. *Landsc. Urban Plan.* **2012**, *106*, 62–72. [CrossRef]

88. Cao, X.; Chen, J.; Imura, H.; Higashi, O. A SVM-based method to extract urban areas from DMSP-OLS and SPOT VGT data. *Remote Sens. Environ.* **2009**, *113*, 2205–2209. [CrossRef]

89. Jing, W.; Yang, Y.; Yue, X.; Zhao, X. Mapping Urban Areas with Integration of DMSP/OLS Nighttime Light and MODIS Data Using Machine Learning Techniques. *Remote Sens.* **2015**, *7*, 12419–12439. [CrossRef]

90. Lu, D.; Tian, H.; Zhou, G.; Ge, H. Regional mapping of human settlements in southeastern China with multisensor remotely sensed data. *Remote Sens. Environ.* **2008**, *112*, 3668–3679. [CrossRef]

91. Dou, Y.; Liu, Z.; He, C.; Yue, H. Urban Land Extraction Using VIIRS Nighttime Light Data: An Evaluation of Three Popular Methods. *Remote Sens.* **2017**, *9*, 175. [CrossRef]

92. Lo, C. Modeling the population of China using DMSP operational linescan system nighttime data. *Photogramm. Eng. Remote Sens.* **2001**, *67*, 1037–1047.

93. Zhuo, L.; Ichinose, T.; Zheng, J.; Chen, J.; Shi, P.J.; Li, X. Modelling the population density of China at the pixel level based on DMSP/OLS non-radiance-calibrated night-time light images. *Int. J. Remote Sens.* **2009**, *30*, 1003–1018. [CrossRef]

94. Sutton, P.C.; Elvidge, C.D.; Ghosh, T. Estimation of gross domestic product at sub-national scales using nighttime satellite imagery. *Int. J. Ecol. Econ. Stat.* **2007**, *8*, 5–21.

95. Ebener, S.; Murray, C.; Tandon, A.; Elvidge, C.C. From wealth to health: modelling the distribution of income per capita at the sub-national level using night-time light imagery. *Int. J. Health Geogr.* **2005**, *4*, 5. [CrossRef]

96. Takahashi, K.I.; Terakado, R.; Nakamura, J.; Daigo, I.; Matsuno, Y.; Adachi, Y. In-Use Stock of Copper Analysis Using Satellite Nighttime Light Observation Data. *Mater. Trans.* **2009**, *50*, 1871–1874. [CrossRef]

97. Tian, J.; Zhao, N.; Samson, E.L.; Wang, S. Brightness of nighttime lights as a proxy for freight traffic: A case study of China. *IEEE J. Sel. Top. Appl. Earth Obs. Remote Sens.* **2014**, *7*, 206–212. [CrossRef]

98. Zhu, X.; Ma, M.; Yang, H.; Ge, W. Modeling the Spatiotemporal Dynamics of Gross Domestic Product in China Using Extended Temporal Coverage Nighttime Light Data. *Remote Sens.* **2017**, *9*, 626. [CrossRef]

99. Lal-Tabak, A. *Identifying Bias in Luminosity-Based Estimation: A Local Level Assessment of Night Light Data as a Proxy for Economic Activity*; Northwestern University: Evanston, IL, USA, 2019.

100. Ghosh, T.; Powell, R.L.; Elvidge, C.D.; Baugh, K.E.; Sutton, P.C.; Anderson, S. Shedding light on the global distribution of economic activity. *Open Geogr. J.* **2010**, *3*, 147–160.

101. Bennie, J.; Davies, T.W.; Inger, R.; Gaston, K.J.; Chisholm, R. Mapping artificial lightscapes for ecological studies. *Methods Ecol. Evol.* **2014**, *5*, 534–540. [CrossRef]

102. Henderson, J.V.; Storeygard, A.; Weil, D.N. Measuring Economic Growth from Outer Space. *Am. Econ. Rev.* **2012**, *102*, 994–1028. [CrossRef] [PubMed]

103. Xu, H.; Yang, H.; Li, X.; Jin, H.; Li, D. Multi-Scale Measurement of Regional Inequality in Mainland China during 2005–2010 Using DMSP/OLS Night Light Imagery and Population Density Grid Data. *Sustainability* **2015**, *7*, 13469–13499. [CrossRef]

104. Zhou, Y.; Ma, T.; Zhou, C.; Xu, T. Nighttime Light Derived Assessment of Regional Inequality of Socioeconomic Development in China. *Remote Sens.* **2015**, *7*, 1242–1262. [CrossRef]

105. Ge, W.; Yang, H.; Zhu, X.; Ma, M.; Yang, Y. Ghost City Extraction and Rate Estimation in China Based on NPP-VIIRS Night-Time Light Data. *ISPRS Int. Geo-Inf.* **2018**, *7*, 219. [CrossRef]

106. Elvidge, C.D.; Sutton, P.C.; Ghosh, T.; Tuttle, B.T.; Baugh, K.E.; Bhaduri, B.; Bright, E. A global poverty map derived from satellite data. *Comput. Geosci.* **2009**, *35*, 1652–1660. [CrossRef]

107. Wang, W.; Cheng, H.; Zhang, L. Poverty assessment using DMSP/OLS night-time light satellite imagery at a provincial scale in China. *Adv. Space Res.* **2012**, *49*, 1253–1264. [CrossRef]

108. Jean, N.; Burke, M.; Xie, M.; Davis, W.M.; Lobell, D.B.; Ermon, S. Combining satellite imagery and machine learning to predict poverty. *Science* **2016**, *353*, 790–794. [CrossRef] [PubMed]

109. Henderson, J.V.; Squires, T.L.; Storeygard, A.; Weil, D.N. *The Global Spatial Distribution of Economic Activity: Nature, History, and the Role of Trade*; National Bureau of Economic Research: Cambridge, MA, USA, 2016.

110. Ma, T.; Zhou, Y.; Wang, Y.; Zhou, C.; Haynie, S.; Xu, T. Diverse relationships between Suomi-NPP VIIRS night-time light and multi-scale socioeconomic activity. *Remote Sens. Lett.* **2014**, *5*, 652–661. [CrossRef]

111. Doll, C.H.; Muller, J.-P.; Elvidge, C.D. Night-time imagery as a tool for global mapping of socioeconomic parameters and greenhouse gas emissions. *AMBIO* **2000**, *29*, 157–162. [CrossRef]

112. Ma, T. An estimate of the pixel-level connection between Visible Infrared Imaging Radiometer Suite Day/Night Band (VIIRS DNB) nighttime lights and land features across China. *Remote Sens.* **2018**, *10*, 723. [CrossRef]

113. Ma, T. Quantitative responses of satellite-derived nighttime lighting signals to anthropogenic land-use and land-cover changes across China. *Remote Sens.* **2018**, *10*, 1447. [CrossRef]

114. Keola, S.; Andersson, M.; Hall, O. Monitoring economic development from space: using nighttime light and land cover data to measure economic growth. *World Dev.* **2015**, *66*, 322–334. [CrossRef]

115. Ma, T. Multi-Level Relationships between Satellite-Derived Nighttime Lighting Signals and Social Media–Derived Human Population Dynamics. *Remote Sens.* **2018**, *10*, 1128. [CrossRef]

116. Li, X.; Chen, F.; Chen, X. Satellite-observed nighttime light variation as evidence for global armed conflicts. *IEEE J. Sel. Top. Appl. Earth Obs. Remote Sens.* **2013**, *6*, 2302–2315. [CrossRef]

117. Li, X.; Li, D. Can night-time light images play a role in evaluating the Syrian Crisis? *Int. J. Remote Sens.* **2014**, *35*, 6648–6661. [CrossRef]

118. Li, X.; Li, D.; Xu, H.; Wu, C. Intercalibration between DMSP/OLS and VIIRS night-time light images to evaluate city light dynamics of Syria's major human settlement during Syrian Civil War. *Int. J. Remote Sens.* **2017**, *38*, 5934–5951. [CrossRef]

119. Jiang, W.; He, G.; Long, T.; Liu, H. Ongoing conflict makes Yemen dark: From the perspective of nighttime light. *Remote Sens.* **2017**, *9*, 798. [CrossRef]

120. Li, X.; Zhang, R.; Huang, C.; Li, D. Detecting 2014 Northern Iraq Insurgency using night-time light imagery. *Int. J. Remote Sens.* **2015**, *36*, 3446–3458. [CrossRef]

121. Li, X.; Liu, S.; Jendryke, M.; Li, D.; Wu, C. Night-Time Light Dynamics during the Iraqi Civil War. *Remote Sens.* **2018**, *10*, 858. [CrossRef]

122. Gillespie, T.W.; Frankenberg, E.; Fung Chum, K.; Thomas, D. Night-time lights time series of tsunami damage, recovery, and economic metrics in Sumatra, Indonesia. *Remote Sens. Lett.* **2014**, *5*, 286–294. [CrossRef]

123. Elliott, R.J.R.; Strobl, E.; Sun, P. The local impact of typhoons on economic activity in China: A view from outer space. *J. Urban Econ.* **2015**, *88*, 50–66. [CrossRef]

124. Olshansky, R.B.; Hopkins, L.D.; Johnson, L.A. Disaster and recovery: Processes compressed in time. *Nat. Hazards Rev.* **2012**, *13*, 173–178. [CrossRef]

125. Cao, C.; Shao, X.; Uprety, S. Detecting light outages after severe storms using the S-NPP/VIIRS day/night band radiances. *IEEE Geosci. Remote Sens. Lett.* **2013**, *10*, 1582–1586. [CrossRef]

126. Zhao, X.; Yu, B.; Liu, Y.; Yao, S.; Lian, T.; Chen, L.; Yang, C.; Chen, Z.; Wu, J. NPP-VIIRS DNB Daily Data in Natural Disaster Assessment: Evidence from Selected Case Studies. *Remote Sens.* **2018**, *10*, 1526. [CrossRef]

127. Croft, T.A. Nighttime images of the earth from space. *Sci. Am.* **1978**, *239*, 86–101. [CrossRef]

128. Kiyofuji, H.; Saitoh, S.-I. Use of nighttime visible images to detect Japanese common squid Todarodes pacificus fishing areas and potential migration routes in the Sea of Japan. *Mar. Ecol. Prog. Ser.* **2004**, *276*, 173–186. [CrossRef]

129. Cho, K.; Ito, R.; Shimoda, H.; Sakata, T. Technical note and cover Fishing fleet lights and sea surface temperature distribution observed by DMSP/OLS sensor. *Int. J. Remote Sens.* **1999**, *20*, 3–9. [CrossRef]

130. Waluda, C.M.; Griffiths, H.J.; Rodhouse, P.G. Remotely sensed spatial dynamics of the Illex argentinus fishery, Southwest Atlantic. *Fish Res.* **2008**, *91*, 196–202. [CrossRef]

131. Waluda, C.M.; Trathan, P.N.; Elvidge, C.D.; Hobson, V.R.; Rodhouse, P.G. Throwing light on straddling stocks of Illex argentinus: Assessing fishing intensity with satellite imagery. *Can. J. Fish. Aquat. Sci.* **2002**, *59*, 592–596. [CrossRef]

132. Paulino, C.; Aroni, E.; Xu, H.; Alburqueque, E.; Demarcq, H. Use of nighttime visible images in the study of the spatial and temporal variability of fishing areas of jumbo flying squid (Dosidicus gigas) outside Peruvian EEZ 2004–2015. *Fish Res.* **2017**, *191*, 144–153. [CrossRef]

133. Elvidge, C.; Zhizhin, M.; Baugh, K.; Hsu, F.-C. Automatic Boat Identification System for VIIRS Low Light Imaging Data. *Remote Sens.* **2015**, *7*, 3020–3036. [CrossRef]

134. Geronimo, R.; Franklin, E.; Brainard, R.; Elvidge, C.; Santos, M.; Venegas, R.; Mora, C. Mapping Fishing Activities and Suitable Fishing Grounds Using Nighttime Satellite Images and Maximum Entropy Modelling. *Remote Sens.* **2018**, *10*, 1604. [CrossRef]

135. Syarifudin, U.; Salman, D.; Alam Ali, S. Application of Viirs-Dnb Satellite Data to Detect Ship Distribution Patterns, Fishing Activity Index and Planning Instrument of Pelagic Capture Fisheries in Bone Bay Waters. *Int. J. Sci. Res.* **2017**, *6*, 693–702.

136. Elvidge, C.D.; Ghosh, T.; Baugh, K.; Zhizhin, M.; Hsu, F.-C.; Katada, N.S.; Penalosa, W.; Hung, B.Q. Rating the Effectiveness of Fishery Closures with Visible Infrared Imaging Radiometer Suite Boat Detection Data. *Front. Mar. Sci.* **2018**, *5*, 132. [CrossRef]

137. Liu, Y.; Saitoh, S.-I.; Hirawake, T. Detection of squid and pacific saury fishing vessels around Japan using VIIRS Day/Night Band image. *Proc. Asia-Pac. Adv. Netw.* **2015**, *39*, 28–39. [CrossRef]

138. Cabral, R.B.; Mayorga, J.; Clemence, M.; Lynham, J.; Koeshendrajana, S.; Muawanah, U.; Nugroho, D.; Anna, Z.; Mira; Ghofar, A.; et al. Rapid and lasting gains from solving illegal fishing. *Nat. Ecol. Evol.* **2018**, *2*, 650–658. [CrossRef] [PubMed]

139. Elvidge, C.D.; Baugh, K.; Zhizhin, M.; Hsu, F.; Ghosh, T. Supporting international efforts for detecting illegal fishing and GAS flaring using viirs. In Proceedings of the 2017 IEEE International Geoscience and Remote Sensing Symposium (IGARSS), Fort Worth, TX, USA, 23–28 July 2017; pp. 2802–2805.

140. Hsu, F.-C.; Elvidge, C.D.; Baugh, K.; Zhizhin, M.; Ghosh, T.; Kroodsma, D.; Susanto, A.; Budy, W.; Riyanto, M.; Nurzeha, R. Cross-Matching VIIRS Boat Detections with Vessel Monitoring System Tracks in Indonesia. *Remote Sens.* **2019**, *11*, 995. [CrossRef]

141. Amaral, S.; Câmara, G.; Monteiro, A.M.V.; Quintanilha, J.A.; Elvidge, C.D. Estimating population and energy consumption in Brazilian Amazonia using DMSP night-time satellite data. *Comput. Environ. Urban Syst.* **2005**, *29*, 179–195. [CrossRef]

142. Malte, M.; Nicolai, M.; William, H.; Raper, S.C.B.; Katja, F.; Reto, K.; Frame, D.J.; Allen, M.R. Greenhouse-gas emission targets for limiting global warming to 2 degrees C. *Nature* **2009**, *458*, 1158–1162.

143. Ou, J.; Liu, X.; Li, X.; Chen, Y. Quantifying the relationship between urban forms and carbon emissions using panel data analysis. *Landsc. Ecol.* **2013**, *28*, 1889–1907. [CrossRef]

144. Elvidge, C.D.; Baugh, K.E.; Kihn, E.A.; Kroehl, H.W.; Davis, E.R.; Davis, C.W. Relation between satellite observed visible-near infrared emissions, population, economic activity and electric power consumption. *Int. J. Remote Sens.* **1997**, *18*, 1373–1379. [CrossRef]

145. Shi, K.; Yu, B.; Huang, Y.; Hu, Y.; Yin, B.; Chen, Z.; Chen, L.; Wu, J. Evaluating the Ability of NPP-VIIRS Nighttime Light Data to Estimate the Gross Domestic Product and the Electric Power Consumption of China at Multiple Scales: A Comparison with DMSP-OLS Data. *Remote Sens.* **2014**, *6*, 1705–1724. [CrossRef]

146. Chand, T.R.K.; Badarinath, K.V.S.; Elvidge, C.D.; Tuttle, B.T. Spatial characterization of electrical power consumption patterns over India using temporal DMSP-OLS night-time satellite data. *Int. J. Remote Sens.* **2009**, *30*, 647–661. [CrossRef]

147. Oda, T.; Maksyutov, S. A very high-resolution (1 km × 1 km) global fossil fuel CO_2 emission inventory derived using a point source database and satellite observations of nighttime lights. *Atmos. Chem. Phys.* **2011**, *11*, 543–556. [CrossRef]

148. Ghosh, T.; Elvidge, C.D.; Sutton, P.C.; Baugh, K.E.; Ziskin, D.; Tuttle, B.T. Creating a Global Grid of Distributed Fossil Fuel CO_2 Emissions from Nighttime Satellite Imagery. *Energies* **2010**, *3*, 1895–1913. [CrossRef]

149. Shi, K.; Chen, Y.; Li, L.; Huang, C. Spatiotemporal variations of urban CO_2 emissions in China: A multiscale perspective. *Appl. Energy* **2018**, *211*, 218–229. [CrossRef]

150. Townsend, A.C.; Bruce, D.A. The use of night-time lights satellite imagery as a measure of Australia's regional electricity consumption and population distribution. *Int. J. Remote Sens.* **2010**, *31*, 4459–4480. [CrossRef]

151. Xie, Y.; Weng, Q. World energy consumption pattern as revealed by DMSP-OLS nighttime light imagery. *GISci. Remote Sens.* **2015**, *53*, 265–282. [CrossRef]

152. Zhizhin, M.N.; Elvidge, C.; Baugh, K.; Hsu, F.C. Five years of gas flaring by country, oil field or flare observed by the Suomi NPP satellite. In Proceedings of the AGU Fall Meeting, San Francisco, CA, USA, 12–16 December 2016.

153. Shi, K.; Chen, Y.; Yu, B.; Xu, T.; Yang, C.; Li, L.; Huang, C.; Chen, Z.; Liu, R.; Wu, J. Detecting spatiotemporal dynamics of global electric power consumption using DMSP-OLS nighttime stable light data. *Appl. Energy* **2016**, *184*, 450–463. [CrossRef]

154. Letu, H.; Hara, M.; Tana, G.; Nishio, F. A saturated light correction method for DMSP/OLS nighttime satellite imagery. *IEEE Trans. Geosci. Remote Sens.* **2012**, *50*, 389–396. [CrossRef]

155. Entekhabi, D.; Letu, H.; Bao, Y.; Tana, G.; Hara, M.; Nishio, F.; Honda, Y.; Sawada, H.; Shi, J.; Oki, T. Relationship between DMSP/OLS nighttime light and CO_2 emission from electric power plant. *Land Surf. Remote Sens.* **2012**, *8524*, 85242G.

156. Ou, J.; Liu, X.; Li, X.; Shi, X. Mapping Global Fossil Fuel Combustion CO_2 Emissions at High Resolution by Integrating Nightlight, Population Density, and Traffic Network Data. *IEEE J. Sel. Top. Appl. Earth Obs. Remote Sens.* **2016**, *9*, 1674–1684. [CrossRef]

157. Zhao, N.; Samson, E.L.; Currit, N.A. Nighttime-Lights-Derived Fossil Fuel Carbon Dioxide Emission Maps and Their Limitations. *Photogramm. Eng. Remote Sens.* **2015**, *81*, 935–943. [CrossRef]

158. Ou, J.; Liu, X.; Li, X.; Li, M.; Li, W. Evaluation of NPP-VIIRS Nighttime Light Data for Mapping Global Fossil Fuel Combustion CO_2 Emissions: A Comparison with DMSP-OLS Nighttime Light Data. *PLoS ONE* **2015**, *10*, e0138310. [CrossRef]

159. Lu, H.; Liu, G. Spatial effects of carbon dioxide emissions from residential energy consumption: A county-level study using enhanced nocturnal lighting. *Appl. Energy* **2014**, *131*, 297–306. [CrossRef]

160. Lo, C.P. Urban Indicators of China from Radiance-Calibrated Digital DMSP-OLS Nighttime Images. *Ann. Assoc. Am. Geogr.* **2002**, *92*, 225–240. [CrossRef]

161. Cao, X.; Wang, J.; Chen, J.; Shi, F. Spatialization of electricity consumption of China using saturation-corrected DMSP-OLS data. *Int. J. Appl. Earth Obs. Geoinf.* **2014**, *28*, 193–200. [CrossRef]

162. Xie, Y.; Weng, Q. Detecting urban-scale dynamics of electricity consumption at Chinese cities using time-series DMSP-OLS (Defense Meteorological Satellite Program-Operational Linescan System) nighttime light imageries. *Energy* **2016**, *100*, 177–189. [CrossRef]

163. He, C.; Ma, Q.; Li, T.; Yang, Y.; Liu, Z. Spatiotemporal dynamics of electric power consumption in Chinese Mainland from 1995 to 2008 modeled using DMSP/OLS stable nighttime lights data. *J. Geogr. Sci.* **2012**, *22*, 125–136. [CrossRef]

164. He, C.; Ma, Q.; Liu, Z.; Zhang, Q. Modeling the spatiotemporal dynamics of electric power consumption in Mainland China using saturation-corrected DMSP/OLS nighttime stable light data. *Int. J. Digit. Earth* **2013**, *7*, 993–1014. [CrossRef]

165. Shi, K.; Chen, Y.; Yu, B.; Xu, T.; Chen, Z.; Liu, R.; Li, L.; Wu, J. Modeling spatiotemporal CO_2 (carbon dioxide) emission dynamics in China from DMSP-OLS nighttime stable light data using panel data analysis. *Appl. Energy* **2016**, *168*, 523–533. [CrossRef]

166. Su, Y.; Chen, X.; Li, Y.; Liao, J.; Ye, Y.; Zhang, H.; Huang, N.; Kuang, Y. China's 19-year city-level carbon emissions of energy consumptions, driving forces and regionalized mitigation guidelines. *Renew. Sust. Energ. Rev.* **2014**, *35*, 231–243. [CrossRef]

167. Shi, K.; Yu, B.; Zhou, Y.; Chen, Y.; Yang, C.; Chen, Z.; Wu, J. Spatiotemporal variations of CO_2 emissions and their impact factors in China: A comparative analysis between the provincial and prefectural levels. *Appl. Energy* **2019**, *233–234*, 170–181. [CrossRef]

168. Shi, K.; Yu, B.; Huang, C.; Wu, J.; Sun, X. Exploring spatiotemporal patterns of electric power consumption in countries along the Belt and Road. *Energy* **2018**, *150*, 847–859. [CrossRef]

169. Shi, K.; Yang, Q.; Fang, G.; Yu, B.; Chen, Z.; Yang, C.; Wu, J. Evaluating spatiotemporal patterns of urban electricity consumption within different spatial boundaries: A case study of Chongqing, China. *Energy* **2019**, *167*, 641–653. [CrossRef]

170. Hara, M.; Okada, S.; Yagi, H.; Moriyama, T.; Shigehara, K.; Sugimori, Y. Progress for stable artificial lights distribution extraction accuracy and estimation of electric power consumption by means of DMSP/OLS nighttime imagery. *Int. J. Remote Sens. Earth Sci.* **2004**, *1*, 31–42.

171. Letu, H.; Hara, M.; Yagi, H.; Naoki, K.; Tana, G.; Nishio, F.; Shuhei, O. Estimating energy consumption from night-time DMPS/OLS imagery after correcting for saturation effects. *Int. J. Remote Sens.* **2010**, *31*, 4443–4458. [CrossRef]

172. Liu, X.; Ou, J.; Wang, S.; Li, X.; Yan, Y.; Jiao, L.; Liu, Y. Estimating spatiotemporal variations of city-level energy-related CO_2 emissions: An improved disaggregating model based on vegetation adjusted nighttime light data. *J. Clean Prod.* **2018**, *177*, 101–114. [CrossRef]

173. Meng, L.; Graus, W.; Worrell, E.; Huang, B. Estimating CO_2 (carbon dioxide) emissions at urban scales by DMSP/OLS (Defense Meteorological Satellite Program's Operational Linescan System) nighttime light imagery: Methodological challenges and a case study for China. *Energy* **2014**, *71*, 468–478. [CrossRef]

174. Elvidge, C.; Ziskin, D.; Baugh, K.; Tuttle, B.; Ghosh, T.; Pack, D.; Erwin, E.; Zhizhin, M. A Fifteen Year Record of Global Natural Gas Flaring Derived from Satellite Data. *Energies* **2009**, *2*, 595–622. [CrossRef]

175. Elvidge, C.; Zhizhin, M.; Baugh, K.; Hsu, F.-C.; Ghosh, T. Methods for Global Survey of Natural Gas Flaring from Visible Infrared Imaging Radiometer Suite Data. *Energies* **2016**, *9*, 14. [CrossRef]

176. Blasing, T.J.; Hand, K. Monthly carbon emissions from natural-gas flaring and cement manufacture in the United States. *Tellus* **2010**, *59*, 15–21. [CrossRef]

177. Longcore, T.; Rich, C. Ecological light pollution. *Front. Ecol. Environ.* **2004**, *2*, 191–198. [CrossRef]

178. Katz, Y.; Levin, N. Quantifying urban light pollution—A comparison between field measurements and EROS-B imagery. *Remote Sens. Environ.* **2016**, *177*, 65–77. [CrossRef]

179. Xiang, W.; Tan, M. Changes in Light Pollution and the Causing Factors in China's Protected Areas, 1992–2012. *Remote Sens.* **2017**, *9*, 1026. [CrossRef]

180. Estrada-García, R.; García-Gil, M.; Acosta, L.; Bará, S.; Sanchez-de-Miguel, A.; Zamorano, J. Statistical modelling and satellite monitoring of upward light from public lighting. *Lighting Res. Technol.* **2016**, *48*, 810–822. [CrossRef]

181. Zamorano, J.; de Miguel, A.S.; Ocaña, F.; Pila-Diez, B.; Castaño, J.G.; Pascual, S.; Tapia, C.; Gallego, J.; Fernández, A.; Nievas, M. Testing sky brightness models against radial dependency: A dense two dimensional survey around the city of Madrid, Spain. *J. Quant. Spectrosc. Radiat. Transf.* **2016**, *181*, 52–66. [CrossRef]

182. Kuechly, H.U.; Kyba, C.C.; Ruhtz, T.; Lindemann, C.; Wolter, C.; Fischer, J.; Hölker, F. Aerial survey and spatial analysis of sources of light pollution in Berlin, Germany. *Remote Sens. Environ.* **2012**, *126*, 39–50. [CrossRef]

183. Han, P.; Huang, J.; Li, R.; Wang, L.; Hu, Y.; Wang, J.; Huang, W. Monitoring Trends in Light Pollution in China Based on Nighttime Satellite Imagery. *Remote Sens.* **2014**, *6*, 5541–5558. [CrossRef]

184. Jiang, W.; He, G.; Long, T.; Wang, C.; Ni, Y.; Ma, R. Assessing Light Pollution in China Based on Nighttime Light Imagery. *Remote Sens.* **2017**, *9*, 135. [CrossRef]

185. Butt, M.J. Estimation of Light Pollution Using Satellite Remote Sensing and Geographic Information System Techniques. *GISci. Remote Sens.* **2013**, *49*, 609–621. [CrossRef]

186. Bennie, J.; Davies, T.W.; Duffy, J.P.; Inger, R.; Gaston, K.J. Contrasting trends in light pollution across Europe based on satellite observed night time lights. *Sci. Rep.* **2014**, *4*, 3789. [CrossRef] [PubMed]

187. Cinzano, P.; Falchi, F.; Elvidge, C.D. The first world atlas of the artificial night sky brightness. *Mon. Not. Roy. Astron. Soc.* **2001**, *328*, 689–707. [CrossRef]

188. Kyba, C.C.; Kuester, T.; De Miguel, A.S.; Baugh, K.; Jechow, A.; Hölker, F.; Bennie, J.; Elvidge, C.D.; Gaston, K.J.; Guanter, L. Artificially lit surface of Earth at night increasing in radiance and extent. *Sci. Adv.* **2017**, *3*, e1701528. [CrossRef] [PubMed]

189. Hu, Z.; Hu, H.; Huang, Y. Association between nighttime artificial light pollution and sea turtle nest density along Florida coast: A geospatial study using VIIRS remote sensing data. *Environ. Pollut.* **2018**, *239*, 30–42. [CrossRef] [PubMed]

190. Bennie, J.; Duffy, J.; Davies, T.; Correa-Cano, M.; Gaston, K. Global Trends in Exposure to Light Pollution in Natural Terrestrial Ecosystems. *Remote Sens.* **2015**, *7*, 2715–2730. [CrossRef]

191. Freitas, J.R.; Bennie, J.; Mantovani, W.; Gaston, K.J. Exposure of tropical ecosystems to artificial light at night: Brazil as a case study. *PLoS ONE* **2017**, *12*, e0171655. [CrossRef] [PubMed]

192. Koen, E.L.; Minnaar, C.; Roever, C.L.; Boyles, J.G. Emerging threat of the 21st century lightscape to global biodiversity. *Glob. Chang. Biol.* **2018**, *24*, 2315–2324. [CrossRef] [PubMed]

193. Gaston, K.J.; Duffy, J.P.; Bennie, J. Quantifying the erosion of natural darkness in the global protected area system. *Conserv. Biol.* **2015**, *29*, 1132–1141. [CrossRef]

194. Davies, T.W.; Duffy, J.P.; Bennie, J.; Gaston, K.J. Stemming the Tide of Light Pollution Encroaching into Marine Protected Areas. *Conserv. Lett.* **2016**, *9*, 164–171. [CrossRef]

195. Kamrowski, R.L.; Limpus, C.; Moloney, J.; Hamann, M. Coastal light pollution and marine turtles: assessing the magnitude of the problem. *Endanger. Species Res.* **2012**, *19*, 85–98. [CrossRef]

196. Cabrera-Cruz, S.A.; Smolinsky, J.A.; Buler, J.J. Light pollution is greatest within migration passage areas for nocturnally-migrating birds around the world. *Sci. Rep.* **2018**, *8*, 3261. [CrossRef] [PubMed]

197. La Sorte, F.A.; Fink, D.; Buler, J.J.; Farnsworth, A.; Cabrera-Cruz, S.A. Seasonal associations with urban light pollution for nocturnally migrating bird populations. *Glob. Chang. Biol.* **2017**, *23*, 4609–4619. [CrossRef]

198. Bauer, S.E.; Wagner, S.E.; Burch, J.; Bayakly, R.; Vena, J.E. A case-referent study: light at night and breast cancer risk in Georgia. *Int. J. Health Geogr.* **2013**, *12*, 23. [CrossRef]

199. Kloog, I.; Haim, A.; Stevens, R.G.; Barchana, M.; Portnov, B.A. Light at night co-distributes with incident breast but not lung cancer in the female population of Israel. *Chronobiol. Int.* **2008**, *25*, 65–81. [CrossRef] [PubMed]

200. James, P.; Bertrand, K.A.; Hart, J.E.; Schernhammer, E.S.; Tamimi, R.M.; Laden, F. Outdoor Light at Night and Breast Cancer Incidence in the Nurses' Health Study II. *Environ. Health Perspect.* **2017**, *125*, 087010. [CrossRef]

201. Rybnikova, N.; Stevens, R.G.; Gregorio, D.I.; Samociuk, H.; Portnov, B.A. Kernel density analysis reveals a halo pattern of breast cancer incidence in Connecticut. *Spat. Spatio-Temporal Epidemiol.* **2018**, *26*, 143–151. [CrossRef]

202. Portnov, B.A.; Stevens, R.G.; Samociuk, H.; Wakefield, D.; Gregorio, D.I. Light at night and breast cancer incidence in Connecticut: An ecological study of age group effects. *Sci. Total Environ.* **2016**, *572*, 1020–1024. [CrossRef]

203. Koo, Y.S.; Song, J.-Y.; Joo, E.-Y.; Lee, H.-J.; Lee, E.; Lee, S.-K.; Jung, K.-Y. Outdoor artificial light at night, obesity, and sleep health: Cross-sectional analysis in the KoGES study. *Chronobiol. Int.* **2016**, *33*, 301–314. [CrossRef] [PubMed]

204. Rybnikova, N.A.; Portnov, B.A. Outdoor light and breast cancer incidence: A comparative analysis of DMSP and VIIRS-DNB satellite data. *Int. J. Remote Sens.* **2016**, *38*, 5952–5961. [CrossRef]

205. Garcia-Saenz, A.; Sanchez de Miguel, A.; Espinosa, A.; Valentin, A.; Aragones, N.; Llorca, J.; Amiano, P.; Martin Sanchez, V.; Guevara, M.; Capelo, R.; et al. Evaluating the Association between Artificial Light-at-Night Exposure and Breast and Prostate Cancer Risk in Spain (MCC-Spain Study). *Environ. Health Perspect.* **2018**, *126*, 047011. [CrossRef] [PubMed]

206. Rybnikova, N.; Portnov, B.A. Population-level study links short-wavelength nighttime illumination with breast cancer incidence in a major metropolitan area. *Chronobiol. Int.* **2018**, *35*, 1198–1208. [CrossRef]

207. Huss, A.; van Wel, L.; Bogaards, L.; Vrijkotte, T.; Wolf, L.; Hoek, G.; Vermeulen, R. Shedding Some Light in the Dark—A Comparison of Personal Measurements with Satellite-Based Estimates of Exposure to Light at Night among Children in the Netherlands. *Environ. Health Perspect.* **2019**, *127*, 067001. [CrossRef] [PubMed]

208. Zhang, Q.; Pandey, B.; Seto, K.C. A Robust Method to Generate a Consistent Time Series from DMSP/OLS Nighttime Light Data. *IEEE Trans. Geosci. Remote Sens.* **2016**, *54*, 5821–5831. [CrossRef]

209. Wu, J.; He, S.; Peng, J.; Li, W.; Zhong, X. Intercalibration of DMSP-OLS night-time light data by the invariant region method. *Int. J. Remote Sens.* **2013**, *34*, 7356–7368. [CrossRef]

210. Pandey, B.; Joshi, P.K.; Seto, K.C. Monitoring urbanization dynamics in India using DMSP/OLS night time lights and SPOT-VGT data. *Int. J. Appl. Earth Obs. Geoinf.* **2013**, *23*, 49–61. [CrossRef]

211. Li, X.; Chen, X.; Zhao, Y.; Xu, J.; Chen, F.; Li, H. Automatic intercalibration of night-time light imagery using robust regression. *Remote Sens. Lett.* **2013**, *4*, 45–54. [CrossRef]

212. Tuttle, B.; Anderson, S.; Elvidge, C.; Ghosh, T.; Baugh, K.; Sutton, P. Aladdin's Magic Lamp: Active Target Calibration of the DMSP OLS. *Remote Sens.* **2014**, *6*, 12708–12722. [CrossRef]

213. Pandey, B.; Zhang, Q.; Seto, K.C. Comparative evaluation of relative calibration methods for DMSP/OLS nighttime lights. *Remote Sens. Environ.* **2017**, *195*, 67–78. [CrossRef]

214. Zhang, Q.; Schaaf, C.; Seto, K.C. The Vegetation Adjusted NTL Urban Index: A new approach to reduce saturation and increase variation in nighttime luminosity. *Remote Sens. Environ.* **2013**, *129*, 32–41. [CrossRef]

215. Liu, X.; Hu, G.; Chen, Y.; Li, X.; Xu, X.; Li, S.; Pei, F.; Wang, S. High-resolution multi-temporal mapping of global urban land using Landsat images based on the Google Earth Engine Platform. *Remote Sens. Environ.* **2018**, *209*, 227–239. [CrossRef]

216. Goodchild, M. Citizens as sensors: The world of volunteered geography. *GeoJournal* **2007**, *69*, 211–221. [CrossRef]

217. Xie, Y.; Weng, Q. Spatiotemporally enhancing time-series DMSP/OLS nighttime light imagery for assessing large-scale urban dynamics. *ISPRS-J. Photogramm. Remote Sens.* **2017**, *128*, 1–15. [CrossRef]

218. Small, C.; Elvidge, C.D.; Baugh, K. Mapping urban structure and spatial connectivity with VIIRS and OLS night light imagery. In Proceedings of the Urban Remote Sensing Event (JURSE), Sao Paulo, Brazil, 21–23 April 2013; pp. 230–233.

219. Falchi, F.; Cinzano, P.; Duriscoe, D.; Kyba, C.C.; Elvidge, C.D.; Baugh, K.; Portnov, B.A.; Rybnikova, N.A.; Furgoni, R. The new world atlas of artificial night sky brightness. *Sci. Adv.* **2016**, *2*, e1600377. [CrossRef] [PubMed]

220. Bará, S.; Rodríguez-Arós, Á.; Pérez, M.; Tosar, B.; Lima, R.C.; Sánchez de Miguel, A.; Zamorano, J. Estimating the relative contribution of streetlights, vehicles, and residential lighting to the urban night sky brightness. *Lighting Res. Technol.* **2017**. [CrossRef]

221. Xie, Y.; Weng, Q.; Weng, A. A comparative study of NPP-VIIRS and DMSP-OLS nighttime light imagery for derivation of urban demographic metrics. In Proceedings of the Earth Observation and Remote Sensing Applications (EORSA), Changsha, China, 11–14 June 2014; pp. 335–339.

222. Jing, X.; Shao, X.; Cao, C.; Fu, X.; Yan, L. Comparison between the Suomi-NPP Day-Night Band and DMSP-OLS for Correlating Socio-Economic Variables at the Provincial Level in China. *Remote Sens.* **2015**, *8*, 17. [CrossRef]

223. Zhang, X.; Wu, J.; Peng, J.; Cao, Q. The Uncertainty of Nighttime Light Data in Estimating Carbon Dioxide Emissions in China: A Comparison between DMSP-OLS and NPP-VIIRS. *Remote Sens.* **2017**, *9*, 797. [CrossRef]

224. Elvidge, C.; Hsu, F.-C.; Baugh, K.; Ghosh, T. National Trends in Satellite-Observed Lighting: 1992–2012. In *Global Urban Monitoring and Assessment through Earth Observation*; CRC Press: Boca Raton, FL, USA, 2014; pp. 97–120.

225. Shao, X.; Cao, C.; Zhang, B.; Qiu, S.; Elvidge, C.; Von Hendy, M. Radiometric calibration of DMSP-OLS sensor using VIIRS day/night band. In Proceedings of the Earth Observing Missions and Sensors: Development, Implementation, and Characterization III, Beijing, China, 13–16 October 2014; p. 92640A.

226. Zheng, Q.; Weng, Q.; Wang, K. Developing a new cross-sensor calibration model for DMSP-OLS and Suomi-NPP VIIRS night-light imageries. *ISPRS-J. Photogramm. Remote Sens.* **2019**, *153*, 36–47. [CrossRef]

227. Zhao, M.; Cheng, W.; Liu, Q.; Wang, N. Spatiotemporal measurement of urbanization levels based on multiscale units: A case study of the Bohai Rim Region in China. *J. Geogr. Sci.* **2016**, *26*, 531–548. [CrossRef]

228. Small, C.; Pozzi, F.; Elvidge, C. Spatial analysis of global urban extent from DMSP-OLS night lights. *Remote Sens. Environ.* **2005**, *96*, 277–291. [CrossRef]

229. He, C.; Liu, Z.; Tian, J.; Ma, Q. Urban expansion dynamics and natural habitat loss in China: A multiscale landscape perspective. *Glob. Chang. Biol.* **2014**, *20*, 2886–2902. [CrossRef] [PubMed]

230. Liu, X.; Hu, G.; Ai, B.; Li, X.; Shi, Q. A Normalized Urban Areas Composite Index (NUACI) Based on Combination of DMSP-OLS and MODIS for Mapping Impervious Surface Area. *Remote Sens.* **2015**, *7*, 17168–17189. [CrossRef]

231. Liu, Y.; Hu, C.; Zhan, W.; Sun, C.; Murch, B.; Ma, L. Identifying industrial heat sources using time-series of the VIIRS Nightfire product with an object-oriented approach. *Remote Sens. Environ.* **2018**, *204*, 347–365. [CrossRef]

232. Ma, T.; Zhou, Y.; Zhou, C.; Haynie, S.; Pei, T.; Xu, T. Night-time light derived estimation of spatio-temporal characteristics of urbanization dynamics using DMSP/OLS satellite data. *Remote Sens. Environ.* **2015**, *158*, 453–464. [CrossRef]

233. Small, C.; Elvidge, C.D. Night on Earth: Mapping decadal changes of anthropogenic night light in Asia. *Int. J. Appl. Earth Obs. Geoinf.* **2013**, *22*, 40–52. [CrossRef]

234. Kyba, C.C.; Wagner, J.M.; Kuechly, H.U.; Walker, C.E.; Elvidge, C.D.; Falchi, F.; Ruhtz, T.; Fischer, J.; Holker, F. Citizen science provides valuable data for monitoring global night sky luminance. *Sci. Rep.* **2013**, *3*, 1835. [CrossRef]

235. Sánchez de Miguel, A.; Zamorano, J.; Gómez Castaño, J.; Pascual, S. Evolution of the energy consumed by street lighting in Spain estimated with DMSP-OLS data. *J. Quant. Spectrosc. Radiat. Transf.* **2014**, *139*, 109–117. [CrossRef]

236. Cao, C.; Bai, Y. Quantitative Analysis of VIIRS DNB Nightlight Point Source for Light Power Estimation and Stability Monitoring. *Remote Sens.* **2014**, *6*, 11915–11935. [CrossRef]

237. Coesfeld, J.; Anderson, S.; Baugh, K.; Elvidge, C.; Schernthanner, H.; Kyba, C. Variation of Individual Location Radiance in VIIRS DNB Monthly Composite Images. *Remote Sens.* **2018**, *10*, 1964. [CrossRef]

238. Aubé, M.; Roby, J.; Kocifaj, M. Evaluating potential spectral impacts of various artificial lights on melatonin suppression, photosynthesis, and star visibility. *PLoS ONE* **2013**, *8*, e67798. [CrossRef]

239. Dobler, G.; Ghandehari, M.; Koonin, S.E.; Sharma, M.S. A Hyperspectral Survey of New York City Lighting Technology. *Sensors* **2016**, *16*, 2047. [CrossRef] [PubMed]

240. Sánchez de Miguel, A.; Kyba, C.C.M.; Aubé, M.; Zamorano, J.; Cardiel, N.; Tapia, C.; Bennie, J.; Gaston, K.J. Colour remote sensing of the impact of artificial light at night (I): The potential of the International Space Station and other DSLR-based platforms. *Remote Sens. Environ.* **2019**, *224*, 92–103. [CrossRef]

241. Rybnikova, N.A.; Portnov, B.A. Remote identification of research and educational activities using spectral properties of nighttime light. *ISPRS-J. Photogramm. Remote Sens.* **2017**, *128*, 212–222. [CrossRef]

242. Xie, M.; Jean, N.; Burke, M.; Lobell, D.; Ermon, S. Transfer learning from deep features for remote sensing and poverty mapping. In Proceedings of the Thirtieth AAAI Conference on Artificial Intelligence, Phoenix, AZ, USA, 12–17 February 2016.

243. Ju, Y.; Dronova, I.; Ma, Q.; Zhang, X. Analysis of urbanization dynamics in mainland China using pixel-based night-time light trajectories from 1992 to 2013. *Int. J. Remote Sens.* **2017**, *38*, 6047–6072. [CrossRef]